Eur. Phys. J. D (2014) 68: 297
DOI: 10.1140/epjd/e2014-50436-4

THE EUROPEAN PHYSICAL JOURNAL D

Colloquium

Recent positron-atom cross section measurements and calculations

Luca Chiari[1,a,b] and Antonio Zecca[2]

[1] ARC Centre of Excellence for Antimatter-Matter Studies, School of Chemical and Physical Sciences, Flinders University, GPO Box 2100, Adelaide, 5001 South Australia, Australia
[2] Department of Physics, University of Trento, Via Sommarive 14, 38123 Povo (Trento), Italy

Received 10 June 2014 / Received in final form 13 August 2014
Published online 14 October 2014 –

Abstract. We review recent cross section results for low-energy positron scattering from atomic targets. A comparison of the latest measurements and calculations for positron collisions with the noble gases and a brief update of the newest studies on other atoms is presented. In particular, we provide an overview of the cross sections for elastic scattering, positronium formation, direct and total ionisation, as well as total scattering, at energies typically between about 0.1 and a few hundred eV. We discuss the differences in the current experimental data sets and compare those results to the available theoretical models. Recommended data sets for the total cross section are also reported for each noble gas. A summary of the recent developments in the scattering from other atoms, such as atomic hydrogen, the alkali and alkaline-earth metals, and two-electron systems is finally provided.

1 Introduction

Electron scattering phenomena play a relevant role in various processes that occur in many scientific disciplines, such as atomic physics, plasma physics, gaseous electronics, astrophysics, and atmospheric chemistry and physics [1]. A knowledge of the cross sections for all those different processes is crucial for a correct modelling and understanding of those phenomena. Total cross sections (TCSs), which give the total scattering probability, for low-energy electron collisions with atoms and molecules, have been measured since the 1920s [2,3]. Good-quality, comprehensive data sets, that are also consistent among independent laboratories, are currently available for electron impact with a wide variety of atomic and molecular targets [4].

Similar to the electron, its anti-particle (the positron) also has important scientific and technological applications in a large variety of fields. A thorough presentation of the many applications of positrons can be found, for instance, in the book by Charlton and Humberston [5]. These include astrophysics, solar physics, bio-medicine (both diagnostics and therapy) and materials science (defect studies and crystallography). From a more fundamental perspective, positrons are essential in the formation of antihydrogen, understanding elementary particle and positronium (Ps) physics, as well as in the investigation of positron binding to ordinary matter, i.e. neutral atoms and molecules. Resonances in electron-impact on atoms and molecules are well-known [6]. However, the situation with respect to positrons is not as clear. On the one hand, positron binding energies have been measured for a large variety of small and large molecules [7,8], although only a few calculations are available [9]. On the other hand, positron-atom binding has long been predicted for many atomic targets [10–12], but it has not been observed yet.

Unlike electron-impact experiments, positron scattering measurements have been hindered by the difficulty in producing a sufficiently intense and monochromatic low-energy beam. Pioneering positron TCS measurements were independently carried out by Costello et al. [13] and Canter et al. [14] in the early 1970s. The first targets to be investigated in those early experiments were simple atomic systems, i.e. mainly the noble gases (see e.g. [15–18]). The reason for this is that those targets are mostly inert species, exist as high-purity atomic gases at room temperature, and are quite inexpensive and readily available. In addition, they represent the relatively easiest systems for theoretical modelling, owing to their closed electronic-shell structure.

Over the following decades, different experimental techniques have progressively been developed in order to undertake more accurate low-energy positron impact studies. As a result, many research groups all over the world have carried out extensive cross section measurements for various kinds of scattering processes. We mention amongst others the groups at University

[a] *Present address*: Department of Physics, Tokyo University of Science, 1-3 Kagurazaka, Shinjuku, Tokyo 162-8601, Japan
[b] e-mail: luca.chiari@flinders.edu.au

College London (UCL) [14], Wayne State University [17], Bielefeld University [18], University of Texas [19], University of Tokyo [20], Yamaguchi University [21], University of California (UCSD) [22], University of Trento [23] and, more recently, the Australian National University (ANU) [24]. In parallel with the rapid growth of experimental data, a variety of different theoretical approaches to model the positron-atom, and successively also positron-molecule, collisional process were being developed [25]. A comprehensive description of the various experimental techniques and theoretical methods employed to investigate positron scattering phenomena was provided in the quite recent review by Surko et al. [26]. We, therefore, do not cover those aspects here again.

In this review, we summarise and compare recent measured and calculated cross sections for positron-atom scattering. We focus on the most recent results for each of the noble gases from He through to Xe in the context of all, earlier and latest, investigations. The reader can also refer to previous review material [1,5,26–30] for a complete discussion of those earlier studies. Results are reported for the TCS and elastic integral cross section (ICS), as well as the Ps formation and ionisation cross sections in the energy range typically from about 0.1 to a few hundred eV. The choice of this energy range is dictated by the fact that the current positron technologies intrinsically impose a lower limit of ∼0.1 eV, while there is a relatively scarce number of experimental and theoretical studies in the intermediate energy range, from 100 to a few thousand eV. In addition to that, we believe that the positron-related physics (such as Ps formation, for instance, or the interplay between the fundamental interactions that drive the scattering dynamics) is likely to be most interesting at energies well below 100 eV. We note here that recent, high-resolution, absolute elastic differential cross sections (DCS) and ICS for the electronic excitations in most of the noble gases have also been measured by the ANU [31–33] and UCSD [34–40] groups. In addition, the existence of cusp-like features or sharp steps in the elastic ICS for the noble gases near the onset of Ps formation was experimentally confirmed by the ANU [41] and Bath [42] groups. These findings evidence the important developments occurred in the positron scattering field over the past decade or so. However, owing to space constraints we will not cover those aspects in the present paper. Recommended TCSs based on the latest, most accurate, experimental data sets are also provided in this colloquium for each of the noble gases. Finally, a short overview of the recent developments in positron collisions with other atoms, such as atomic hydrogen, the alkali and alkaline-earth metals, and two-electron systems is also reported.

The outline of this paper is as follows. In Sections 2 to 6 we present and compare a selection of the measured and computed cross sections for each of the nobles gases: helium, neon, argon, krypton and xenon, respectively. A brief overview of the latest studies on other atomic targets is then given in Section 7. Finally, in Section 8, some conclusions are drawn and future perspectives are discussed from the present review.

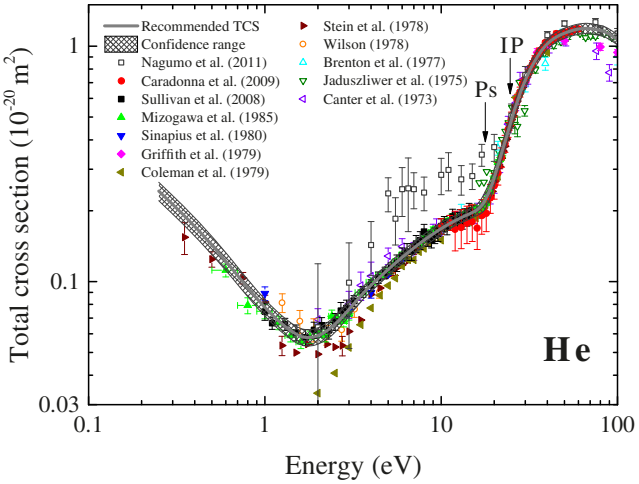

Fig. 1. A selection of the existing TCS measurements for positron scattering from He. Shown are the data of Canter et al. [43], Jaduszliwer et al. [48], Brenton et al. [51], Wilson [52] corrected after Sinapius et al. [18], Stein et al. [53], Coleman et al. [54], Griffith et al. [55], Sinapius et al. [18], Mizogawa et al. [57], Sullivan et al. [24], Caradonna et al. [58] and Nagumo et al. [59]. Also shown is the present recommended TCS and its uncertainty range.

2 Helium

2.1 Total cross section and elastic integral cross section

The study of positron scattering from helium attracted considerable attention from both experimentalists and theoreticians over the years. Helium was among the first targets to be investigated because of its simple structure, on the theoretical side, and its almost ideal properties (stable, non-toxic, non-reactive gas), on the experimental side. Nevertheless, its very small cross section (particularly below ∼10 eV) somewhat complicated the attenuation measurements. In fact, a very long interaction region and a very high pumping speed are typically needed in order to obtain a sufficiently large attenuation of the beam intensity.

In spite of these difficulties, significant effort has been dedicated to positron-helium TCS measurements. Most of those studies were undertaken in the 1970s and 1980s [13,14,18,43–57]. Only more recently, with the advent of brighter, high-resolution spectrometers, has helium gained renewed interest [24,58,59]. Figure 1 shows a comparison of the most recent experimental TCSs for positron scattering from helium [24,58,59] to a selection of earlier results [18,43,48,51–55,57]. Not shown in Figure 1 are the measurements by Karwasz et al. [60] who claimed the presence of resonant-like structures in the TCS for He. That experiment was performed with the spectrometer at the University of Trento, which had been designed by Zecca [61]. Zecca [62] challenged those results and ascribed them to flawed experimental procedures. Karwasz et al. [63] later argued this criticism calling for independent experimental verifications. However, subsequent

Table 1. List of some important physico-chemical properties of the noble gases.

	He	Ne	Ar	Kr	Xe
Van der Waals diameter (Å)	2.8	3.08	3.76	4.04	4.32
Static atomic polarisability (a.u.)	1.38	2.67	11.08	16.8	27.16
Positronium formation threshold energy (eV)	17.8	14.76	8.96	7.19	5.33
First ionisation energy (eV)	24.6	21.56	15.76	13.99	12.13
Number of electrons	2	10	18	36	54

measurements carried out at the ANU [24], with a better energy resolution and a much better signal-to-noise ratio, discarded the possibility for the existence of any positron-He structures with an amplitude one order of magnitude smaller than those claimed by Karwasz et al. [60].

The TCSs for He shown in Figure 1 show a general decrease in their magnitude from the lowest investigated energy up to ∼1.8 eV, where a Ramsauer-Townsend minimum is observed. The Ramsauer-Townsend effect is a phenomenon that requires a quantum mechanical description of the interaction of particles [64]. As described by Schiff [65], it may be physically thought of as "a diffraction of the electron [or positron] around the rare-gas atom, in which the wave-function inside the atom is distorted in just such a way that it fits on smoothly to an undistorted wave-function outside." The result is a suppression of the scattered s-partial-wave and a consequent extremely low dip in the TCS. This effect can only occur at low energies where the s-wave phase shift dominates the cross section. The Ramsauer-Townsend effect was first observed in low-energy electron scattering cross sections from the noble gases [2,66], where the scattering cross section possesses a very small magnitude at incident energies near 1 eV [64]. As noted by Kauppila and Stein [1], a net attractive interaction between the incident positron and the target is needed to produce a Ramsauer-Townsend effect. Hence, the polarisation interaction must dominate over the static interaction in positron-He collisions at those low energies. We will find an analogous minimum in the positron TCSs for neon, whereas no such effect is observed for argon, krypton or xenon. As the incident positron energy increases from the Ramsauer-Townsend minimum, the TCS of He starts to rise in magnitude up to the Ps formation threshold (see Tab. 1) where a change in the slope of the TCS is manifest. As the Ps formation channel becomes open, the TCS suddenly increases even more rapidly as a function of the projectile energy. This behaviour in the TCS stresses the relevant role played by this scattering channel in positron scattering from He and, as we will see later on, in general for all the inert gases. As the succeeding inelastic channel, namely direct ionisation, becomes open at 24.6 eV, the TCS continues to rise in magnitude until it reaches a relatively broad maximum at around 60–70 eV and then it starts to slowly fall in magnitude. We observe that the effect of the opening of the electronic excitations in He is not manifest in the TCS. This might be ascribed to the relatively small cross section of those electronic transitions [31]. This is also clearly shown by the comparison between the TCSs and the elastic ICSs below the Ps formation threshold energy, not just in He (see Fig. 2), but also the other noble gases (see Sects. 3–6). We note that He possesses the smallest TCS among all the noble gases: its magnitude at the Ramsauer-Townsend minimum is just $\sim 0.06 \times 10^{-20}$ m^2, while at its maximum it is of the order of 1.2×10^{-20} m^2. From a semi-classical point of view, this can be explained in terms of the small size of the He atom, but it might also reflect the fact that its electron cloud contains just two electrons, as well as its small static atomic polarisability (see Tab. 1).

Figure 1 shows that the agreement between the various experimental TCSs is surprisingly good, especially if we take into account that many of those measurements were carried out in the early times of low positron activity. The level of accord is uniformly good at all incident energies, expect perhaps at the lowest investigated energies where the scatter among the different data sets becomes somewhat larger. Most of the results cluster along a common shape, with the exception of the earlier data of Coleman et al. [54] and the latest measurements by Nagumo et al. [59]. The lower magnitude of the TCS by Coleman et al. [54] might be explained in terms of the worse angular discrimination of their measurement, compared to the other experiments, at those low energies. In fact it is known that the inability to discriminate positrons that are elastically scattered to the very forward angles from those of the primary, unscattered beam (the so-called forward angle scattering effect), can lead to a significant underestimation of the TCS magnitude [74]. On the other hand, the TCS of Nagumo et al. [59] overestimates the magnitude of all the previous measurements, although it appears to agree with the earlier results of the Toronto group [46] (not shown in Fig. 1). The Tokyo University of Science (TUS) data [59] show a greater scatter and larger uncertainties than the other results, which might be due to the very low positron count rate of their magnetic-field-free spectrometer. We also note here the presence of two discontinuities in the earlier data of Stein et al. [53]: the first one at around 1 eV and the second one at ∼3–4 eV. Given that they occur at similar magnitude values, we believe that they might be due to a range switching error in their pressure readings. We finally observe in Figure 1 a general scarcity of data below ∼1 eV, which indicates the difficulty in conducting measurements at such low energies and for a target with such a small TCS magnitude. Further experiments that might help to elucidate the behaviour of the TCS in this energy region would be, therefore, welcome. The very good level of accord between the different measurements shown in Figure 1 suggests that He might be considered the first benchmarked system for

Table 2. Recommended TCSs for positron scattering from He.

Energy (eV)	TCS (10^{-20} m^2)	TCS uncertainty (10^{-20} m^2)
0.25	2.42×10^{-1}	2.2×10^{-2}
0.3	2.13×10^{-1}	1.9×10^{-2}
0.4	1.73×10^{-1}	1.6×10^{-2}
0.5	1.47×10^{-1}	1.3×10^{-2}
0.6	1.23×10^{-1}	1.1×10^{-2}
0.7	1.06×10^{-1}	9.0×10^{-3}
0.8	9.33×10^{-2}	7.8×10^{-3}
0.9	8.33×10^{-2}	6.8×10^{-3}
1	7.52×10^{-2}	6.0×10^{-3}
1.5	5.91×10^{-2}	4.7×10^{-3}
2	5.81×10^{-2}	4.7×10^{-3}
3	7.78×10^{-2}	6.2×10^{-3}
4	9.66×10^{-2}	5.8×10^{-3}
5	1.13×10^{-1}	6.8×10^{-3}
6	1.27×10^{-1}	7.6×10^{-3}
7	1.39×10^{-1}	8.4×10^{-3}
8	1.50×10^{-1}	9.0×10^{-3}
9	1.60×10^{-1}	9.6×10^{-3}
10	1.68×10^{-1}	1.0×10^{-2}
15	1.96×10^{-1}	9.6×10^{-2}
20	2.75×10^{-1}	2.3×10^{-2}
30	7.21×10^{-1}	5.0×10^{-2}
40	1.03	4.9×10^{-2}
50	1.14	5.7×10^{-2}
60	1.18	5.9×10^{-2}
70	1.19	6.0×10^{-2}
80	1.17	5.8×10^{-2}
90	1.13	5.6×10^{-2}
100	1.07	5.3×10^{-2}

positron scattering from atomic targets, as already argued by Surko et al. [26] and Sullivan et al. [24] amongst others.

Starting from the original measured data, we produced a set of TCSs and an uncertainty range on those values for each noble gas (see next sections) in order to provide some "recommended cross sections". The result for He is shown in Figure 1 and the corresponding numerical values are listed in Table 2. The recommended TCS originates from the average of those data sets that do not deviate from the "main sequence", i.e. cluster around a similar cross section value, taking into account the different experimental conditions in which the various measurements were gathered. Discarded from this analysis are those data sets that show too much statistical scatter, lie well outside the uncertainty range of all other sets, suffer from very large forward angle scattering effects or may have been affected by instrumental errors (such as the data of Stein et al. [53], see above). We have also taken into account some of the theoretical results (see below) to determine the recommended TCS and its confidence bound just for He, especially at very low energies (below 1 eV), where the measurements are scarce and more scattered. We found a posteriori that the recommended cross section is quite insensitive to the details of the method used to generate it. The confidence range (1σ) on the recommended TCS

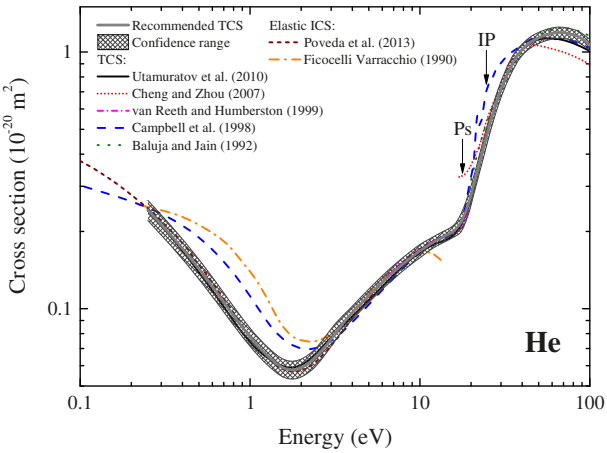

Fig. 2. A selection of the most recent theoretical results for positron scattering from He. Shown are the TCSs computed by Utamuratov et al. [67], Cheng and Zhou [68], Van Reeth and Humberston [69], Campbell et al. [70], Baluja and Jain [71] and the elastic ICSs calculated by Poveda et al. [72] and Ficocelli Varracchio [73]. Also shown is the present recommended TCS and its uncertainty range.

stems from the discrepancy between the various data sets in the "main sequence" and their own uncertainties. We note here that the confidence bound might be wider at the lower incident energies, as statistical uncertainties are typically larger at those low energies.

The level of accord between the recommended TCS and the experimental results plotted in Figure 1 is generally quite good and often to within the confidence level on the present recommended TCS. Exceptions to this observation are the magnetic-field-free measurements of Nagumo et al. [59] and the data of Coleman et al. [54]. In addition, the lower-energy data of Stein et al. [53] seems to somewhat diverge from our recommended TCS. This might be due to an error in their determination of the energy zero. In fact, if the energy scale of the TCSs by Stein et al. [53] was corrected by +0.15 eV, their lower-energy data would fall well within the error band on our recommended TCS. Note that an error of ±0.15 eV in the determination of the energy zero is quite possible in this kind of measurement.The forward angle scattering error might also somewhat contribute to the observed discrepancy, particularly at the lowest incident energies.

Helium has also been extensively studied from a theoretical perspective over the years. In fact numerous calculated TCSs and elastic ICSs have been reported since the late 1960s [58,67–73,75–94]. The very large number of these theoretical studies possibly makes He the most investigated target using positrons as the scattering probe. We note here that the aforementioned theoretical activity started before any experimental data became available. Figure 2 shows a selection of the most recently computed TCSs and elastic ICSs for positron collisions with He. Plotted in Figure 2 are the TCS of Utamuratov et al. [67] calculated using the convergent close-coupling (CCC) method with two-centre expansions, the higher energy TCS of Cheng and Zhou [68] obtained with the

momentum-space coupled-channel optical method, the ab initio TCS of Van Reeth and Humberston [69] calculated using a variant of the Kohn variational method, that of Campbell et al. [70] resulting from their extension of coupled-state theory to two-electron targets and the TCS of Baluja and Jain [71] at energies above 20 eV that stems from a complex-optical-potential approach. Given that any scattering that occurs below the Ps formation threshold energy in atoms is purely elastic, we also compare in Figure 2 the above mentioned TCSs to the elastic ICSs of Poveda et al. [72] and Ficocelli Varracchio [73] calculated with their own optical model-potential method.

Figure 2 shows that there is very good agreement among the various theoretical results for He at energies between about 3 eV and the Ps formation energy. The calculated cross sections in that energy range also agree very well with the presently recommended TCS for He. At the lower energies, the models of Ficocelli Varracchio [73] and Campbell et al. [70] diverge from those of Poveda et al. [72] and Utamuratov et al. [67]. Above the Ps formation energy the various theories and the recommended TCS are still in quite good agreement, with the results of Campbell et al. [70] and Cheng and Zhou [68] only partly disagreeing. Overall, the models of Utamuratov et al. [67], Poveda et al. [72], Van Reeth and Humberston [69] and Baluja and Jain [71] are in very good agreement with each other and do the best job at reproducing the existing experimental results plotted in Figure 1. Hence, they were used to generate the recommended TCS. In light of the great improvements in the most recent calculations, He might now be considered a benchmarked system, not just from an experimental, but also a theoretical point of view. This may be true for the TCS at impact energies below 100 eV and possibly within a confidence level of ∼5%.

2.2 Positronium formation cross section

Positronium is an exotic atom consisting of the bound state of an electron and a positron. This system is unstable due to self-annihilation of the two particles into gamma-ray photons. Ps is formed whenever an incident positron (e^+) possesses enough kinetic energy to "knock out" an electron (e^-) from the target (A) and temporary bind to it, leaving the target as a positive ion:

$$e^+ + A \rightarrow A^+ + Ps\,(e^+, e^-). \quad (1)$$

Ps formation is, therefore, considered like a direct ionisation process where the ejected electron, however, gets bound to the incoming positron and they eventually annihilate with each other to produce two or three photons. Total ionisation comprises both the Ps formation and direct ionisation processes. The minimum energy required to form Ps is given by:

$$E_{Ps} = E_i - 6.8\ \text{eV}, \quad (2)$$

where E_i is the first ionisation energy of the target and 6.8 eV is the Ps binding energy [5].

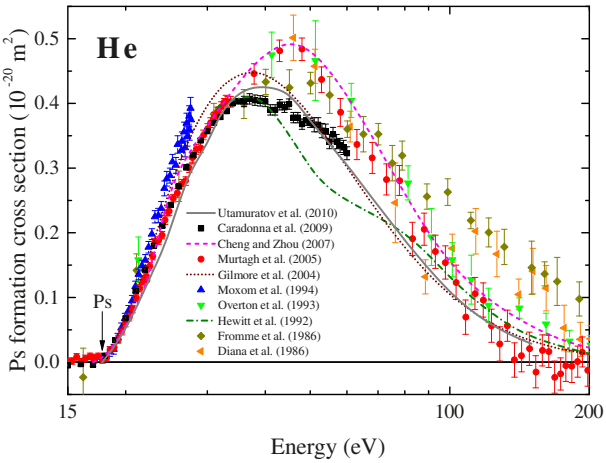

Fig. 3. A selection of the available measured and calculated Ps formation cross sections for positron scattering from He. The experimental results are those of Caradonna et al. [58], Murtagh et al. [102], Moxom et al. [101], Overton et al. [100], Fromme et al. [99] and Diana et al. [98]. The theoretical results are from Utamuratov et al. [67], Cheng and Zhou [68], Gilmore et al. [112] and Hewitt et al. [111].

Ps formation is a significant inelastic scattering channel that is unique to positron impact phenomena. This explains, at least in part, why this scattering channel is so intriguing and interesting to study both experimentally and theoretically. Considerable effort was therefore devoted to measurements of the Ps formation cross section for He [58,95–102]. Ps formation cannot be explained in terms of binary collisions and, hence, modelling its dynamics can be a very challenging task. Nevertheless, a substantial number of theoretical studies has tackled the Ps formation cross section for the simplest many-electron atom [58,67–70,79,92,103–112].

Figure 3 shows a selection of the most recent measurements of the Ps formation cross section for He. The experimental results plotted in Figure 3 include those of Diana et al. [98], Fromme et al. [99], Overton et al. [100], Moxom et al. [101], Murtagh et al. [102] and Caradonna et al. [58]. The agreement between the measurements is very good at the lowest energies, i.e. just after the threshold, but becomes progressively worse as the incident positron energy increases. In fact, at the highest energy, the general level of accord is only marginal. The two most recent measurements, i.e. those of Murtagh et al. [102] and Caradonna et al. [58], agree remarkably well up to ∼33 eV. However, around that energy the cross section of Caradonna et al. [58] seems to level off at about 0.4×10^{-20} m^2 and then decrease in magnitude as the energy increases, while that reported by Murtagh et al. [102] continues to increase in magnitude and reaches a maximum at ∼45 eV. Nevertheless, there is an indication in Figure 3 that the two cross sections might merge again at 70–80 eV. The Ps formation cross section, therefore, seems to reach its maximum between 35 and 45 eV, where it contributes to about half of the observed TCS (see Figs. 1 and 2), and then "turns off" at around 200 eV. The reason for the observed discrepancies among the various measurements

in Figure 3 might lie in the fact that the Ps formation cross sections of Fromme et al. [99], Moxom et al. [101] and Murtagh et al. [102] were extracted from their own measured relative total ionisation cross sections by subtracting previously measured direct ionisation data, after normalising them to the latest electron-impact ionisation data. On the other hand, the results of Diana et al. [98], Overton et al. [100] and Caradonna et al. [58] stem from the direct measurement of the absolute TCS and the fraction of Ps formation relative to total scattering. Marler et al. [22] argued that a relatively small undercounting of direct ionisation events in previous measurements might result in larger Ps formation cross sections for Ar and Kr, as obtained by the UCL group, when taking the difference between total and direct ionisation cross sections (see Sects. 4.2 and 5.2 for more details). This statement was supported by the independent direct ionisation cross section measurements for Ar and Kr of the UCSD group [22,113]. Once their data was subtracted from the UCL total ionisation measurements, the Ps formation cross sections for Ar and Kr obtained in this fashion were in noticeably better agreement with the UCSD Ps formation data. Although no UCSD Ps formation data exist for He to check whether this also the case here, it is reasonable to assume that the same issue persists also in the UCL He measurements. In addition, we note that as a result of their normalisation procedure, Moxom et al. [101], for instance, report a 20% uncertainty on the absolute value of their cross sections. The large scatter in the Ps formation data for He, and most of the other noble gases (see below), does not allow us to devise a unique way which provides a recommended cross section for this scattering channel. Hence, we do not report such cross sections here.

We also present in Figure 3 a choice of the latest theoretical Ps formation cross sections for He. These include the calculation of Hewitt et al. [111] using the close-coupling (CC) approximation, that of Gilmore et al. [112] obtained applying the distorted-wave Born approximation (DWBA), the cross sections by Cheng and Zhou [68] computed with their momentum-space coupled-channel optical method and the CCC results of Utamuratov et al. [67]. There is, in general, a good qualitative agreement among the four theories at all energies. The computations of Hewitt et al. [111] and Gilmore et al. [112] also agree in their magnitude over most of the common energies, while Cheng and Zhou [68] predict a somewhat larger cross section compared to all the other models. The level of accord between the theories and the experiments in Figure 3 is often only qualitative. However, the calculation of Cheng and Zhou [68] seems to do a good job at fitting the experimental data of Murtagh et al. [102], whereas the most recent computation of Utamuratov et al. [67] appears to reproduce quite well the cross sections measured by Caradonna et al. [58].

2.3 Ionisation cross section

Similar to Ps formation, direct ionisation occurs when an incident positron with a sufficient kinetic energy "knocks out" one of the target electrons and leaves the target as a positive ion:

$$e^+ + A \rightarrow e^+ + A^+ + e^-. \quad (3)$$

However, contrary to Ps formation, in this case the ejected electron is free. The minimum energy required to extract an electron from the electron cloud of the target corresponds to the first ionisation energy.

The ionisation cross section for He has been as extensively investigated in the past, just as the Ps formation cross section of that target. However, to the best of our knowledge, there are no recent measurements of the direct ionisation cross section. In fact the latest experiments date back to the early-mid 1990s [114–119], whereas the first measurements were carried out in the preceding decade [99,120–122]. Nonetheless, Murtagh et al. [102] have relatively recently reported some experimental total ionisation cross sections for He. Previous measurements of this cross section were conducted by Moxom et al. [123] and Griffith et al. [95]. We also cite the total double ionisation data of Bluhme et al. [124]. On the theoretical side of things, there are numerous, recent studies of the direct [67,70,90,91,107,109,125–136], as well as the total ionisation cross section [67,70,71,90,107,137].

A selection of the most recent experimental results for the direct ionisation cross section of He is shown in Figure 4. Those results include the single ionisation measurements of Moxom et al. [118], Jacobsen et al. [117] and Knudsen et al. [114], as well as the direct ionisation cross sections of Mori and Sueoka [115] and Fromme et al. [99]. Except for the first measurements by Fromme et al. [99], the level of accord among the various experiments is quite good, in both the shape and magnitude of the cross section, at all common energies. A comparison with Figure 3 shows that the agreement among different laboratories is

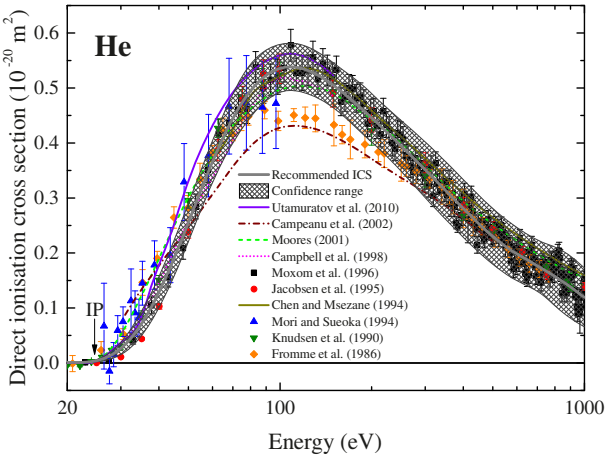

Fig. 4. A selection of the available experimental and theoretical direct ionisation cross sections for positron scattering from He. The measurements are from Fromme et al. [99], Knudsen et al. [114], Mori and Sueoka [115], Jacobsen et al. [117] and Moxom et al. [118], while the calculations are due to Chen and Msezane [132], Campbell et al. [70], Moores [134], Campeanu et al. [129] and Utamuratov et al. [67].

Table 3. Recommended ICSs for direct ionisation in positron-He scattering.

Energy (eV)	ICS (10^{-20} m^2)	ICS uncertainty (10^{-20} m^2)
30	2.15×10^{-2}	1.1×10^{-2}
40	1.24×10^{-1}	2.8×10^{-2}
50	2.55×10^{-1}	3.6×10^{-2}
60	3.69×10^{-1}	3.7×10^{-2}
70	4.50×10^{-1}	4.5×10^{-2}
80	5.00×10^{-1}	5.0×10^{-2}
90	5.28×10^{-1}	4.6×10^{-2}
100	5.40×10^{-1}	4.3×10^{-2}
150	5.06×10^{-1}	4.0×10^{-2}
200	4.46×10^{-1}	4.6×10^{-2}
300	3.51×10^{-1}	5.1×10^{-2}
400	2.81×10^{-1}	5.3×10^{-2}
500	2.29×10^{-1}	5.1×10^{-2}
600	1.96×10^{-1}	4.9×10^{-2}
700	1.82×10^{-1}	5.5×10^{-2}
800	1.69×10^{-1}	5.9×10^{-2}
900	1.42×10^{-1}	5.8×10^{-2}
1000	1.19×10^{-1}	5.4×10^{-2}

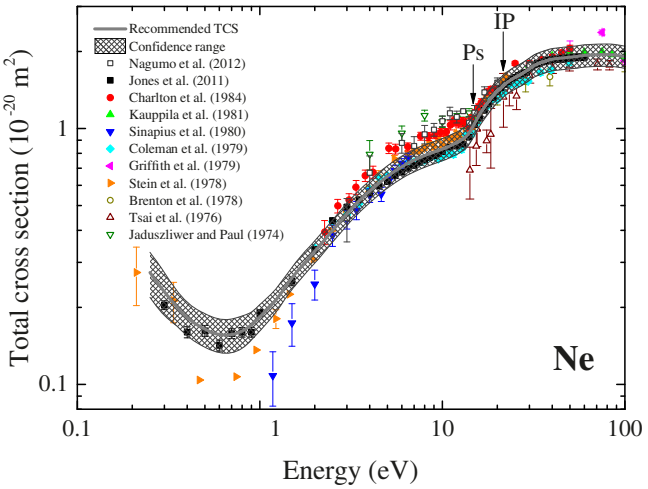

Fig. 5. A selection of the measured TCSs for positron scattering from Ne. Plotted are the results of Jaduszliwer and Paul [138,139], Tsai et al. [140], Brenton et al. [16], Stein et al. [53], Griffith et al. [55], Coleman et al. [54], Sinapius et al. [18], Kauppila et al. [56], Charlton et al. [141], Jones et al. [142] and Nagumo et al. [143]. Also shown is the present recommended TCS and its uncertainty range.

better for the ionisation cross section; this might reflect the greater practical difficulties in the Ps formation measurements. The direct ionisation cross section appears to peak just above 100 eV and it contributes to about 50% of the TCS at that energy. Given that the Ps formation cross section is still about 0.1–0.2$\times 10^{-20}$ m^2 at 100 eV (see Fig. 3), the total ionisation cross section of He appears to constitute a significant fraction (∼60–70%) of the TCS at that energy. The direct ionisation cross section decreases quite slowly as a function of the incident energy after its maximum: at 1000 eV it is still some 20% of the cross section magnitude at its peak.

We report in Figure 4 and in Table 3 our recommended cross sections for direct ionisation in He together with an uncertainty bound on those values. The recommended ICS follows mostly the measured cross sections of Moxom et al. [118], Jacobsen et al. [117] and Knudsen et al. [114]. The data of Fromme et al. [99] are clearly outside the confidence range near threshold and at intermediate energies, possibly because they were the very first of their kind. The data of Mori and Sueoka [115] show quite large statistical scatter and error bars and, hence, lie outside the uncertainty limit at most energies.

Also plotted in Figure 4 is an assortment of the latest theoretical calculations of the direct ionisation cross section for He. They include the CCC computation of Utamuratov et al. [67], the distorted-wave model results of Campeanu et al. [129] and Moores [134] (the latter with close-coupled target states) and the coupled-state calculations of Campbell et al. [70] and Chen and Msezane [132]. All the displayed theories agree quite well with each other, with the experimental data and the recommended ICS at all common energies, with the exception of the model of Campeanu et al. [129]. In effect, this calculation only seems to fit the earlier measurements of Fromme et al. [99], which, in turn, disagree with all the subsequent experiments.

3 Neon

3.1 Total cross section and elastic integral cross section

Similar to the simplest inert atom, neon has also been quite extensively investigated with low-energy positrons. In fact, several TCS measurements have been reported in references [16,18,43,44,49,53–56,138–143]. Plotted in Figure 5 are the most recent experimental results of Jones et al. [142] and Nagumo et al. [143] and some of the previous measurements [16,18,53–56,138–141].

The shape of the TCS for Ne displayed in Figure 5 resembles that for He (Fig. 1), although it is somewhat larger in magnitude. This latter observation was not unexpected, as Ne possesses more electrons than He, its atomic polarisability is bigger and, from a semi-classical perspective, the Ne atom is also larger in size (Tab. 1). Moreover, the Ne TCS displays a Ramsauer-Townsend minimum like in He, although its position in this case is shifted to somewhat lower energies. Despite the scarcity of data below 1 eV, it appears that the aforementioned minimum might be at around 0.6 eV. As the incident energy increases and the Ps formation and, subsequently, the direct ionisation channels become open, the TCS continues to rise with manifest changes in its slope in the proximity of the respective threshold energies (Tab. 1). The relative contribution of the Ps formation channel to the rise in the TCS is evident in Figure 5, although it does not seem as pronounced as in He (Fig. 1). This highlights that the

Ps formation channel in He is relatively stronger than the other scattering channels. The TCS shows a broad maximum at about 70–80 eV with a magnitude of 2×10^{-20} m^2, i.e. larger than the corresponding maximum in He. On the other hand, at the Ramsauer-Townsend minimum the TCS magnitude is just less than 0.2×10^{-20} m^2.

The level of accord among the experimental data shown in Figure 5 is quite good at most common energies. The majority of the measurements share a similar TCS shape, although some of them differ in respect to its magnitude. We note that the earlier results of Jaduszliwer and Paul [138,139], Tsai et al. [140] and Sinapius et al. [18] somewhat diverge from the other data sets at the respective lowest investigated energies. In particular, the data of Sinapius et al. [18] seem to be affected by a large forward angle scattering effect. We note that only the TCS of Jones et al. [142] in Figure 5 has been corrected for the forward angle scattering effect at energies below 13 eV. We also observe in Figure 5 that the two most recent measurements carried out using a magnetised buffer-gas trap and positron beam [142] and a magnetic field-free spectrometer [143], respectively, are not consistent with each other. In fact, the latter experiment reported TCSs that are generally larger than those of the former, although their shapes are similar. This suggests that one of the two measurements might suffer from a systematic error in the determination of the pressure or the length of the interaction region. In addition, the scatter in the data of Nagumo et al. [143] appears to be larger than their error bars. Therefore, further experiments on Ne are needed in order to ascertain the absolute scale of the TCS. This is particularly true at energies below ∼1 eV, where there is a clear scarcity of data.

Plotted in Figure 5 and listed in Table 4 are the present recommended TCSs for positron collisions with Ne. Our recommended TCS agrees quite well with the majority of the experimental results, often to within its confidence range. Exceptions to this observation are the low-energy data of Charlton et al. [141], Sinapius et al. [18], Stein et al. [53], Tsai et al. [140], Jaduszliwer and Paul [138,139] and Nagumo et al. [143] that were not used in the determination of the recommended TCS. We note here that all those measurements belong to the early times of positron research, except for the TUS experiment [143].

A large number of theoretical investigations of the TCS and elastic ICS for positron impact on Ne has been published over the past half-century or so [71,72,75,89,142,144–150]. A selection of the most recent results is shown in Figure 6. These include the TCS of Fursa and Bray [144] calculated using their CCC formalism within the single-centre approximation and the higher-energy TCS of Baluja and Jain [71] obtained with a complex-optical-potential model. Also plotted in Figure 6 are the elastic ICS of Poveda et al. [72] computed using a model-potential approach, that of Jones et al. [142] stemming from a relativistic optical potential model, the many-body calculation of Dzuba et al. [146], the model potential computation of Nakanishi and Schrader [147], the CC calculation by Campeanu and Dubau [148], without the virtual Ps formation channel, and the elastic scattering results of McEachran et al. [149] obtained using the polarised-orbital approximation.

Table 4. Recommended TCSs for positron scattering from Ne.

Energy (eV)	TCS (10^{-20} m^2)	TCS uncertainty (10^{-20} m^2)
0.25	2.74×10^{-1}	5.5×10^{-2}
0.3	2.29×10^{-1}	4.6×10^{-2}
0.4	1.80×10^{-1}	2.7×10^{-2}
0.5	1.64×10^{-1}	2.5×10^{-2}
0.6	1.55×10^{-1}	2.3×10^{-2}
0.7	1.56×10^{-1}	2.3×10^{-2}
0.8	1.61×10^{-1}	2.4×10^{-2}
0.9	1.70×10^{-1}	2.0×10^{-2}
1	1.84×10^{-1}	2.2×10^{-2}
1.5	2.65×10^{-1}	2.7×10^{-2}
2	3.29×10^{-1}	3.3×10^{-2}
3	4.66×10^{-1}	4.7×10^{-2}
4	5.69×10^{-1}	5.7×10^{-2}
5	6.51×10^{-1}	6.5×10^{-2}
6	7.10×10^{-1}	7.1×10^{-2}
7	7.52×10^{-1}	7.5×10^{-2}
8	7.84×10^{-1}	7.8×10^{-2}
9	8.09×10^{-1}	8.1×10^{-2}
10	8.31×10^{-1}	8.3×10^{-2}
15	1.04	0.10
20	1.40	0.14
30	1.71	0.17
40	1.87	0.19
50	1.90	0.19
60	1.94	0.19
70	1.95	0.20
80	1.95	0.20
90	1.95	0.20
100	1.91	0.19

The agreement among the different theories shown in Figure 6 is quite good at energies above ∼1 eV where all the models lie within the confidence range on our recommended TCS, except for the earlier results of McEachran et al. [149] and Nakanishi and Schrader [147], and the higher-energy TCS of Baluja and Jain [71]. The model of Fursa and Bray [144] appears to best represent the most recent TCS measurements on Ne. However, the level of accord among the various theories becomes worse as the incident energy decreases below 1 eV. In fact, the various calculations span a cross section range of up to an order of magnitude at those energies, although they still share a quite similar qualitative behaviour. This disagreement suggests that further development of the current theoretical approaches is warranted particularly at the very low energies. Additional TCS measurements at energies well below 1 eV might also be very helpful in this regard.

3.2 Positronium formation cross section

Measurements of the Ps formation cross section for positron scattering from Ne have been carried out since

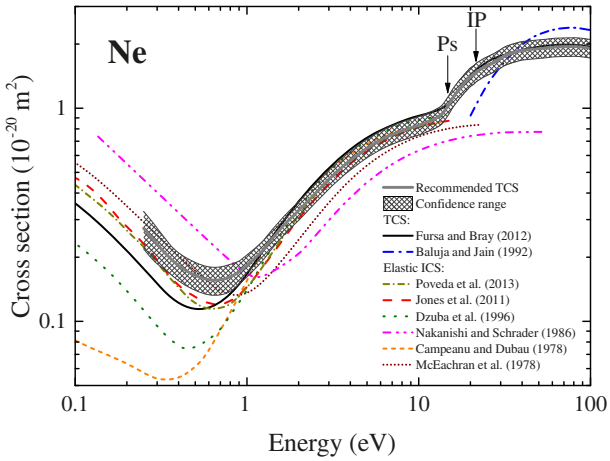

Fig. 6. A selection of the most recent theoretical results for positron scattering from Ne. Shown are the TCSs of Fursa and Bray [144] and Baluja and Jain [71], as well as the elastic ICSs of Poveda et al. [72], Jones et al. [142] (ROP), Dzuba et al. [146], Nakanishi and Schrader [147], Campeanu and Dubau [148] and McEachran et al. [149]. Also shown is the present recommended TCS and its uncertainty range.

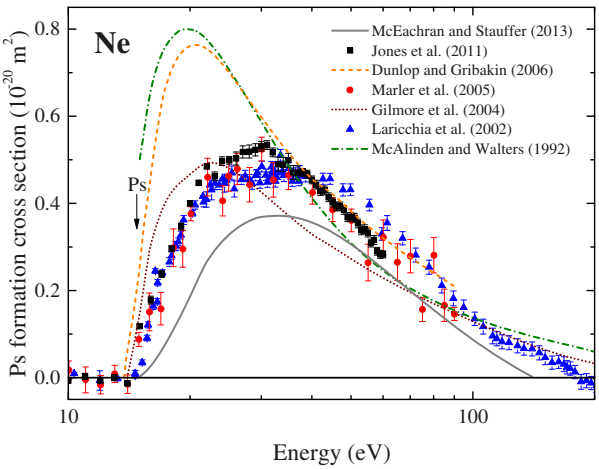

Fig. 7. A selection of some of the Ps formation cross sections for positron-Ne collisions. The measured results are from Jones et al. [142], Marler et al. [113] and Laricchia et al. [151]. The calculated cross sections results are from McEachran and Stauffer [155], Dunlop and Gribakin [156], Gilmore et al. [112] and McAlinden and Walters [92].

the early 1980s [97,101,113,142,151–153]. We show in Figure 7 a selection of those experimental cross sections: Jones et al. [142] and Marler et al. [113] used a strongly magnetised, buffer-gas trap beam, whereas Laricchia et al. [151] employed a mostly electrostatic spectrometer. The data of Marler et al. [113] is more scattered than the other two measurements, however, all the experiments are in good qualitative agreement with each other. Similar to He (see Sect. 2.2), we mention here that the UCL Ne data [151] might also be affected by the systematic error uncovered by Marler et al. [22] in the Ar and Kr data (see Sects. 4.2 and 5.2). Nevertheless, given the good accord we observe in Figure 7, we expect that effect to be small in Ne. The Ps formation cross section for Ne seems to peak at about 30 eV with a magnitude of $\sim 0.5 \times 10^{-20}$ m^2, but we note that there is some scatter among the data sets at around the maximum. The cross section then decreases monotonically from the peak up to about 200 eV where it approaches a zero magnitude, similar to He.

The very first theoretical study of the Ps formation cross section for Ne [154] predates the first measurement on that target by about six years. Nevertheless, other calculations have later been reported in references [92,112,155,156] and these are plotted in Figure 7. McAlinden and Walters [92] calculated the cross section for Ps($2p$) formation in the truncated coupled-static approximation, Gilmore et al. [112] employed the DWBA, while Dunlop and Gribakin [156] performed first-order and all-order computations of Ps formation in the ground-state from valence and subvalence subshells using first-order many-body perturbation theory. Finally, McEachran and Stauffer [155] have recently reported results based upon their ab initio relativistic optical potential method with an additional absorption channel to simulate Ps formation. The level of accord among those four models is, in general, only marginal as they show quite different shapes and magnitudes. However, we note that the results of Dunlop and Gribakin [156] and McAlinden and Walters [92] are somewhat similar to each other. The agreement between the available calculations and the existing experiments is also very marginal and becomes qualitative at the higher energies only.

3.3 Ionisation cross section

A good number of studies has looked into ionisation of Ne by positron impact. The most recent measurements of the direct ionisation cross section have been performed in the early 2000s [113,157], while some earlier experiments have been carried out between the mid-1980s and the late 1990s [114–117,121,158]. For completeness, we also mention the total ionisation measurements of Laricchia et al. [151], Szłuinska et al. [159] and Marler et al. [113], as well as the total double ionisation cross section of Bluhme et al. [124]. Plotted in Figure 8 are some of those direct ionisation results, namely the single-ionisation experiments of Knudsen et al. [114], Jacobsen et al. [117] and Van Reeth et al. [157], and the direct ionisation cross sections of Mori and Sueoka [115] and Marler et al. [113] measured using the time-of-flight method and a magnetised, buffer-gas trap and positron beam, respectively.

We observe in Figure 8 that there is only a qualitative agreement among the various experimental results, as they can differ in their magnitude by up to a factor of 2. In spite of the "noisiness" in the existing data, it seems reasonable to assign a change in the slope of the TCS to the opening of the first ionisation channel (21.56 eV, see Tab. 1). Similar to He (see Fig. 4), the peak in the direct ionisation cross section for Ne is just above 100 eV. The direct ionisation

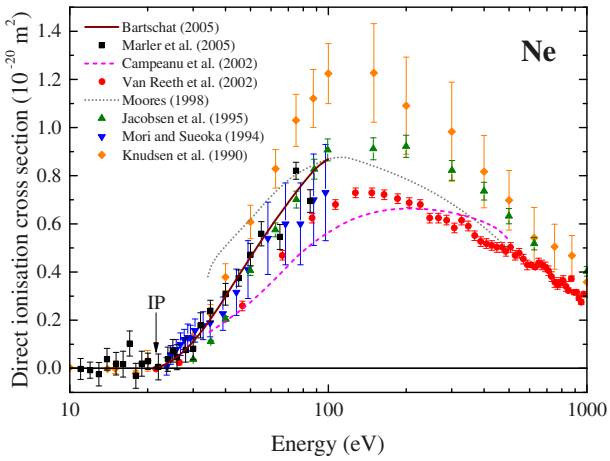

Fig. 8. A comparison of the direct ionisation cross sections for positron impact with Ne. Shown are the data measured by Knudsen et al. [114], Mori and Sueoka [115], Jacobsen et al. [117], Van Reeth et al. [157] and Marler et al. [113]. Also plotted are the calculations of Moores [160], Campeanu et al. [129] and Bartschat [161].

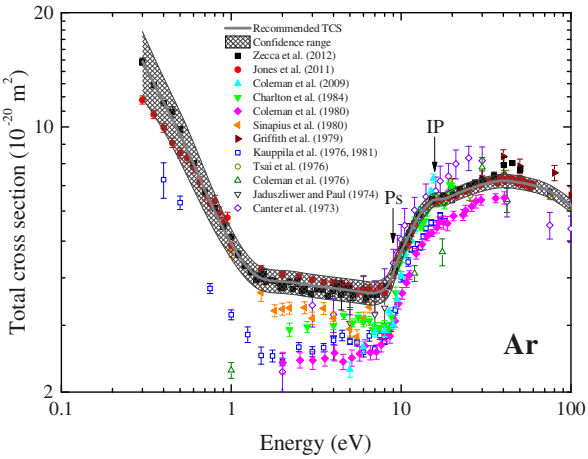

Fig. 9. The available experimental TCSs for positron collisions with argon. Shown are the data of Canter et al. [43,44] Jaduszliwer and Paul [138,139], Kauppila et al. [17,56], Tsai et al. [140], Coleman et al. [49,162,163], Griffith et al. [55], Sinapius et al. [18], Charlton et al. [141], Jones et al. [142], Zecca et al. [164]. Also shown is the present recommended TCS and its uncertainty range.

cross section decreases monotonically as a function of the positron energy, from its maximum up to 1000 eV where its magnitude is still 0.3–0.4 $\times$ 10^{-20} m^2, that is between half and one third of its peak magnitude.

A number of theoretical investigations of the direct ionisation cross section for positron scattering from Ne have been reported [127–130,160,161]. Two calculations of the total ionisation cross section of Ne also appear to exist [71,144]. We compare in Figure 8 a selection of those direct ionisation computations to the above-mentioned experimental work. Shown are the calculation of Moores [160], obtained with a distorted wave method with CC target states, the distorted-wave model result of Campeanu et al. [129] and the hybrid approach of Bartschat [161], using the distorted wave theory coupled to an R-matrix CC expansion. We only find a marginal qualitative agreement among the theories shown in Figure 8, as they generally differ from each other in both shape and magnitude. The behaviour of the calculation by Moores [160] is qualitatively similar to the experimental data. The result of Bartschat [161] does a quite good job at reproducing the magnitude of the experimental results of Marler et al. [113], Jacobsen et al. [117] and Mori and Sueoka [115] below 100 eV. Finally, we note that at energies above ∼300 eV the trend of all the theories seems to agree with the energy dependence of the measured data.

4 Argon

4.1 Total cross section and elastic integral cross section

Argon is possibly the preferred target to measure among the noble gases owing to its ready availability in the Earth's atmosphere (∼1% of the dry atmosphere by volume), which makes it quite inexpensive. In addition, the fact that Ar is bigger in size than either He or Ne means that its cross sections are also relatively larger in magnitude, which facilitates experiments based on the attenuation method. This is reflected in the large number of experimental investigations [17,18,43,44,49,55,56,138–142,162–164] and a similar amount of theoretical studies [71,72,75,89,92,142,144–147,165–170] undertaken with positrons. We note that a complete set of cross sections, including TCS and elastic ICS, as well as Ps formation and direct ionization cross sections, for positron scattering from Ar has been recently reported by McEachran et al. [171]. Given that the experimental data, which are already plotted in Figures 9–12, have been preferentially considered to derive those recommended cross sections, we do not report here the results of McEachran et al. [171].

Figure 9 displays all the existing positron-Ar TCS measurements. The TCSs rapidly decrease in magnitude from the lowest measured energy up to about ∼1.3 eV. This behaviour reflects the relatively large atomic polarisability of Ar, which, at those very low energies, can cause the attractive dipole interaction to overcome the static repulsion. This leads to an overall attractive potential that drives the scattering dynamics and manifests itself in large negative values of the scattering lengths, such as in the heavier noble gases. The TCS continues to decrease in magnitude above ∼1.3 eV but at a slower pace, until it starts to suddenly rise again as the Ps formation and direct ionisation channels progressively become open (see Tab. 1). The TCS reaches a broad maximum at around 40 eV and then starts to decline in magnitude. The shape of the TCS for Ar is quite different to that of He and Ne (see Figs. 1 and 5, respectively), as it does not show a Ramsauer-Townsend minimum like in those

two lighter noble gases. We note that Kauppila et al. [17] did ascribe the minimum in their data to a Ramsauer-Townsend effect and there are actually theoretical predictions for the existence of such an effect in the positron-Ar elastic ICS (see [17,26] and references therein). However, Sullivan et al. [74] argued that the dip at around 2 eV in the Detroit data [17] may simply arise from the effect on the TCS of a poor angular discrimination against forward scattering. We mention here that another mechanism might more likely play a role in producing the wide minimum in the Ar TCS, namely the sum of the various partial cross sections with different energy dependence. As anticipated above, the TCS for Ar is significantly larger in magnitude than that of He and Ne (again see Figs. 1 and 5), by more than one order of magnitude at the low energies. This observation can be easily explained in terms of the much larger atomic polarisability and higher number of electrons in Ar compared to He and Ne. We also observe that the overall shape of the Ar TCS in the range from a few tenths to a few tens of eV has a close resemblance to that of the N_2 TCS (see e.g. [173]).

The agreement between the various measured TCSs shown in Figure 9 is only limited to their shape, as their magnitude varies significantly from one another. This discrepancy, particularly at the lower energies, is mainly due to the different angular discriminations of the spectrometers used in those experiments, which, in turn, leads to different forward angle scattering corrections. We note that only the data of Jones et al. [142] have been corrected for the forward angle scattering effect up to 15 eV. We also observe that the TCSs of Zecca et al. [164] and Jones et al. [142] are generally larger in magnitude than the other data sets, which reflects the superior angular discrimination of those two experiments. The slight difference in the magnitude of those two TCSs is mostly accounted for by the forward scattering effect affecting the Trento data [164], so that once the latter are corrected for that effect, those two measurements are actually in very good agreement with each other. Exception to this observation is the energy region below 0.6 eV, where the ANU data are clearly too low in magnitude. The very good level of accord between those two data sets also suggests that positron-Ar might be considered a nearly benchmarked system at the TCS level, at least above ∼0.6 eV. It is also worth noting in Figure 9 that the data of Canter et al. [43,44] and Griffith et al. [55] are somewhat larger in magnitude than either the Trento [164] or ANU [142] results, for TCSs above the first ionisation energy, although most of that discrepancy might be accounted for if the overall uncertainties on the experiments are considered.

We show in Figure 9 and list in Table 5 the present recommended TCSs for positron impact with Ar. That TCS mostly resembles the behaviour of the data measured at the ANU because they are corrected for the forward angle scattering effect. However, below 0.6 eV where the ANU data are clearly too low in magnitude, the recommended TCS follows the Trento measurements. Although the latter cross sections are uncorrected for the forward scattering effect, which means that the real TCS would be somewhat larger in magnitude than the Trento results, they currently represent the best TCSs at those energies. The recommended TCS lies above most of the earlier measurements, particularly at the lower energies, with the exception of the data of Canter et al. [43,44] and Griffith et al. [55] (see above).

Table 5. Recommended TCSs for positron scattering from Ar.

Energy (eV)	TCS (10^{-20} m^2)	TCS uncertainty (10^{-20} m^2)
0.3	14.86	2.97
0.4	11.64	1.78
0.5	9.55	1.43
0.6	8.00	1.14
0.7	6.77	0.86
0.8	5.94	0.67
0.9	5.36	0.53
1	4.89	0.43
1.5	3.94	0.28
2	3.91	0.27
3	3.82	0.27
4	3.75	0.26
5	3.72	0.26
6	3.66	0.26
7	3.64	0.25
8	3.73	0.26
9	4.12	0.29
10	4.70	0.27
15	6.38	0.27
20	6.58	0.26
30	7.07	0.28
40	7.28	0.29
50	7.14	0.29
60	7.02	0.28
70	6.90	0.28
80	6.68	0.27
90	6.42	0.26
100	6.20	0.25

A selection of the recent computations at the TCS and elastic ICS level for positron collisions with Ar is given in Figure 10. Shown are the TCSs calculated by Nahar and Wadehra [169] using the relativistic Dirac equation, that of Baluja and Jain [71] who employed a complex-optical-potential approach, that of Parcell et al. [170] determined with the polarized-orbital method and a distorted-wave framework, and that of Fursa and Bray [144] which was determined within the CCC formulation in the single-centre approximation. Also displayed in Figure 10 are the elastic ICSs of Schrader [89], Datta et al. [167], Nakanishi and Schrader [147], Jain [168] and Poveda et al. [72], obtained with their own model potential method, that of McEachran et al. [166] computed within the polarised-orbital approximation, the many-body theory of Dzuba et al. [146] and the calculation of Jones et al. [142] under the relativistic optical potential approach.

Figure 10 shows that there is a clear scatter in the magnitude of the existing calculations, although they seem

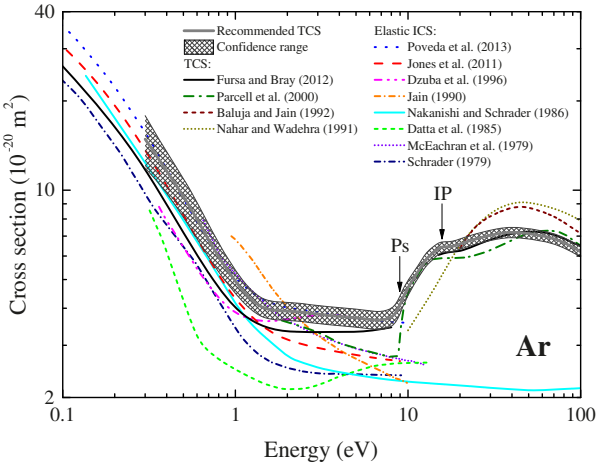

Fig. 10. Some of the latest calculations for positron scattering from argon. Plotted are the TCSs of Nahar and Wadehra [169] (CP), Baluja and Jain [71], Parcell et al. [170] and Fursa and Bray [144], as well as the elastic ICSs of Schrader [89], McEachran et al. [166], Datta et al. [167], Nakanishi and Schrader [147], Jain [168] (PCP2), Dzuba et al. [146], Jones et al. [142] (ROP) and Poveda et al. [72]. Also shown is the present recommended TCS and its uncertainty range.

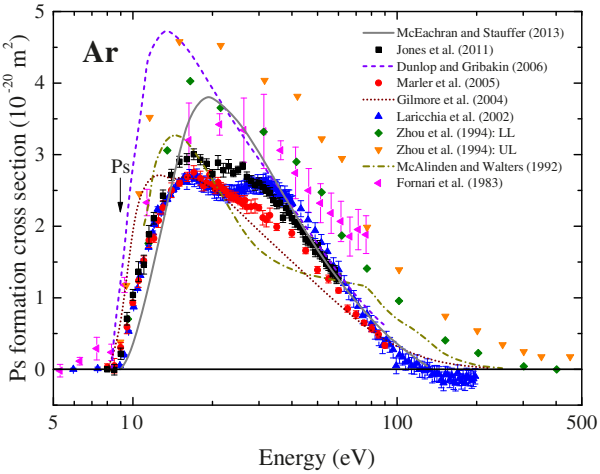

Fig. 11. A comparison of the measured and computed Ps formation cross sections for positron impact with argon. Shown are the data of Fornari et al. [96], Laricchia et al. [151], Marler et al. [113] and Jones et al. [142], as well as the upper (UL) and lower (LL) limit on the cross section reported by Zhou et al. [172]. Also given are the theoretical results of McAlinden and Walters [92], Gilmore et al. [112], Dunlop and Gribakin [156] and McEachran and Stauffer [155].

to share a somewhat analogous qualitative behaviour, namely a rapid fall in the cross section from the lowest energy up to the Ps formation threshold with a slow-down in the decrease rate just above 1 eV. Interestingly, the cross section range spanned by the calculations appears to match the scatter in the experimental data, such as to indicate that the theoretical approaches might have progressively improved as more accurate measurements became available. However, the calculations generally tend to underestimate the most recent data, especially above 1 eV (see Fig. 9). The computations that best reproduce the present recommended TCS and the most recent experimental results [142,164] are that of Poveda et al. [72] below the Ps formation threshold, that of Parcell et al. [170] between that inelastic threshold and the first ionisation potential and that of Fursa and Bray [144] above that latter inelastic threshold energy. Once again, we note that those three calculations are among the most recent, which suggests that a significant progress in the positron scattering theory for this target has been achieved.

4.2 Positronium formation cross section

Given the bulk of studies reporting the TCS and elastic ICS for positron scattering from Ar, it is not surprising to find that analogous effort has been put over the years into investigating Ps formation from that target. This is demonstrated by the significant amount of experimental [22,39,96,97,101,113,142,151,152,172,174,175] and, to a lesser extent, theoretical [92,112,154–156] work on the Ps formation cross sections for the positron-Ar system. Figure 11 compares some of those measured and calculated results.

The experimental cross sections shown in Figure 11 are those of Jones et al. [142] and Marler et al. [113], obtained using a strongly magnetised, buffer-gas trap and positron beam, and those of Laricchia et al. [151], Fornari et al. [96] and Zhou et al. [172], who employed a mostly electrostatic spectrometer. We note that the Ps formation cross sections reported by Laricchia et al. [151] were extracted from their own total ionisation cross sections and other available data, whereas all the other experiments involve direct absolute Ps formation cross section measurements. In addition, Zhou et al. [172] only determined upper and lower limits on the Ps formation cross section.

The agreement between the various experiments is only modest at best. The cross sections of Fornari et al. [96] and Zhou et al. [172] are significantly larger in magnitude than the other results at all positron impact energies. From threshold up to about 15 eV there is good quantitative agreement between the measurements of Laricchia et al. [151], Marler et al. [113] and Jones et al. [142]. The accord between the two former data sets persists up to and including the peak in the cross section. The maximum occurs at around 15 eV with a magnitude of 2.5–3 $\times$ 10^{-20} m^2, that is much larger than in either He or Ne (see Figs. 3 and 7). This is easily explained in terms of the larger number of electrons and the larger atomic polarisability in Ar. However, the data of Laricchia et al. [151], Marler et al. [113] and Jones et al. [142] diverge at higher energies until they tend to merge again at around several tens of eV. The results of Laricchia et al. [151], in particular, show a second peak in the cross section, which they ascribe to Ps formation in excited states and/or by capture of electrons in the inner sub-shells of Ar. However, that second peak is not present in any of the other measurements that, instead, decrease

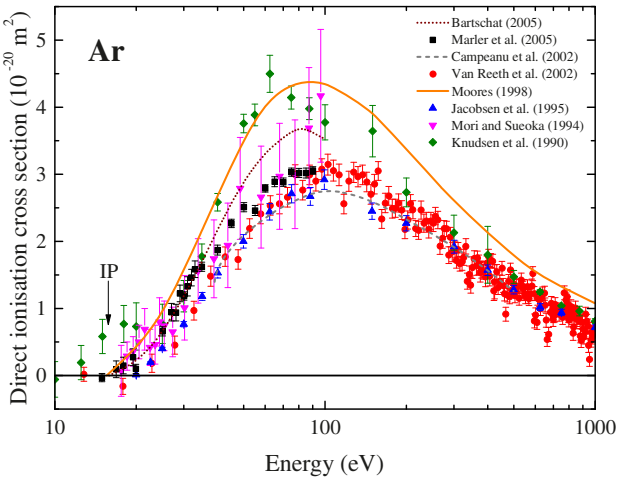

Fig. 12. A selection of the available direct ionisation cross sections for positron impact with argon. Plotted are the measurements of Knudsen et al. [114], Mori and Sueoka [115], Jacobsen et al. [117], Van Reeth et al. [157] and Marler et al. [113]. Also shown are the calculations by Moores [160], Campeanu et al. [129] and Bartschat [161].

monotonically with energy after the maximum. Marler et al. [22] argued that the aforementioned second peak in the Laricchia et al. [151] data might be an artefact due to their method that relies on measured ionisation data. In fact, Marler et al. [22] have shown that by subtracting their measured direct ionisation cross sections from the total ionisation cross sections reported by Laricchia et al. [151], it is possible to reconcile the Ps formation cross section obtained in this fashion with their own results. Finally, the three data sets of Laricchia et al. [151], Marler et al. [113] and Jones et al. [142] seem to indicate that the Ps formation cross section might reach a zero magnitude just above 100 eV, that is at a much smaller (nearly half) incident positron energy compared to He and Ne (again see Figs. 3 and 7).

The theoretical results plotted in Figure 11 belong to McAlinden and Walters [92], who calculated the cross sections for Ps($1s$) formation in the truncated coupled-static approximation, Gilmore et al. [112] with their DWBA approach, Dunlop and Gribakin [156], who computed first-order and all-order Ps formation in the ground-state from valence and subvalence subshells employing first-order many-body perturbation theory, and McEachran and Stauffer [155], who applied their ab initio relativistic optical potential method with an additional absorption channel to simulate Ps formation. The four calculations fail at reproducing the shape and the magnitude of the measured cross sections after the threshold and around the peak. This suggests that further development of the theoretical approaches in this energy range may be needed. However, above 40 eV the latest two computations [155,156] exhibit an energy dependence that is very similar to that of the data of Laricchia et al. [151], Marler et al. [113] and Jones et al. [142]. This level of accord is also quantitative with the experiments by Laricchia et al. [151] and Jones et al. [142].

4.3 Ionisation cross section

Measurements of the direct ionisation cross section for positron impact with Ar have been undertaken with a strongly magnetised buffer-gas trap and positron beam [113], as well as mostly electrostatic spectrometers [114–118,121,157]. Total ionisation cross sections for positron-Ar have also been reported from experiments using the two different techniques [113,123,151,176]. We show in Figure 12 some of those experimental cross sections for the ionisation of Ar by positron impact, namely the single ionisation data of Knudsen et al. [114], Jacobsen et al. [117] and Van Reeth et al. [157], and the direct ionisation results of Mori and Sueoka [115] and Marler et al. [113].

The agreement between the various measurements plotted in Figure 12 is quite good, in terms of both the shape and magnitude of the cross section. The only exception to this statement is the earlier data of Knudsen et al. [114] that significantly overestimate the magnitude of all the other experimental results around the peak and at the threshold. The maximum in the direct ionisation cross section appears to be at around 100 eV with a magnitude that is about half that of the TCS at that energy (see Fig. 9). This highlights the importance of this inelastic channel in the scattering process at those positron energies. We note that the peak cross section for ionisation in Ar is much larger in magnitude than in either He or Ne (Figs. 4 and 8). Similar to the Ps formation cross section, this is again consistent with its bigger number of target electrons and larger atomic polarisability. We also observe in Figure 12 that the cross section decreases monotonically after the peak and that, although approaching a zero magnitude, it is still non-zero at 1000 eV.

There appear to be only two calculations of the total ionisation cross section for positron scattering from Ar in references [71,144], while there are quite a few calculations of the direct ionisation cross section [127–130,160,161]. Figure 12 shows some of those direct ionisation computations and compares them to the recent experimental work. Specifically, plotted in that figure are the distorted wave results with CC target states of Moores [160], the distorted-wave computation by Campeanu et al. [129] and the calculation of Bartschat [161] with the distorted-wave formalism together with an R-matrix CC expansion. We find a good qualitative agreement between those calculations and the measurements shown in Figure 12. That level of accord becomes quantitative between the data of Marler et al. [113] and the model of Bartschat [161] from threshold up to ∼35 eV, and between the three most recent experiments and the theoretical approach of Campeanu et al. [129] at most common energies.

5 Krypton

5.1 Total cross section and elastic integral cross section

Because the Earth's atmosphere contains so little krypton and isolating it takes so much energy, krypton is

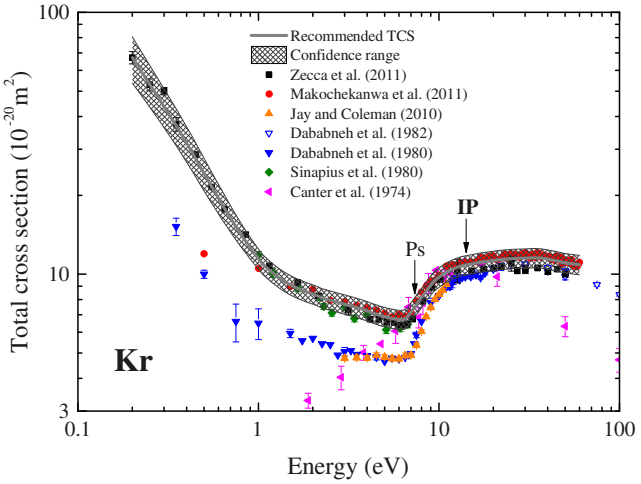

Fig. 13. Measured TCSs for positron impact with krypton: Canter et al. [43,44], Sinapius et al. [18], Dababneh et al. [177,178], Jay and Coleman [179], Makochekanwa et al. [32], Zecca et al. [180]. Also shown is the present recommended TCS and its uncertainty range.

fairly expensive. Nevertheless, for reasons similar to those leading at investigating Ar, Kr has attracted significant attention by the atomic collision community. In this regard, we mention the availability of both TCS measurements [18,32,43,44,177–180] and calculations at the TCS [71,144,170] and elastic ICS level [32,72,75,89,181–183] for positron scattering from Kr.

A picture representing the existing positron-Kr TCS measurements is given in Figure 13. The shape of the Kr TCS somewhat resembles that of Ar (see Fig. 9), as it dramatically falls in magnitude from the lowest energy up to the Ps formation energy, with a manifest change in the slope just above 1 eV. As we noted in Ar, this qualitative trend is likely to be due to the relatively significant atomic polarisability of the target (see Tab. 1). With the onset of the Ps formation channel, and later direct ionisation, the TCS rapidly rises in magnitude until it peaks at about 35 eV. The shape of the Kr TCS rules out the possibility of a Ramsauer-Townsend effect: similar to the Ar TCS, the presence of a minimum is most likely to be due to the different energy dependence of the contributing partial cross sections. A comparison of Figure 13 with Figure 9 reveals that the magnitude of the Kr TCS is much larger than that for Ar at all common incident energies and, in particular, at the lower energies, where it can be as much as a factor of 3 greater. This observation is consistent with the ∼50% larger polarisability and double the number of electrons in Kr compared to Ar.

There is a good qualitative level of accord between the TCS measurements shown in Figure 13, except for the data of Canter et al. [43,44], which exhibit a quite different behaviour. We note that only the ANU data [32] are corrected for the forward angle scattering effect and that their lowest energy point appears to be somewhat too low in magnitude. In analogy to Ar (Fig. 9), the difference between the ANU [32], Trento [180] and, to a lesser extent, Bielefeld [18] measurements is due to the different forward scattering errors affecting those three experiments. However, those three data sets become all consistent once the angular correction is taken into account. Figure 13 shows that the TCSs of Dababneh et al. [177], Jay and Coleman [179] and Canter et al. [43,44] diverge from the three aforementioned data sets as the incident energy decreases. This behaviour might reflect the inferior angular discrimination of those experiments. It is also worth noting that the TCS of Dababneh et al. [177] shares the same overall shape with the two most recent measurements.

Table 6. Recommended TCSs for positron collisions with Kr.

Energy (eV)	TCS (10^{-20} m^2)	TCS uncertainty (10^{-20} m^2)
0.2	67.17	13.43
0.3	43.83	7.42
0.4	31.76	4.90
0.5	24.19	3.49
0.6	19.44	2.52
0.7	16.35	1.86
0.8	14.17	1.46
0.9	12.49	1.17
1	11.15	0.95
1.5	8.97	0.74
2	8.32	0.72
3	7.67	0.63
4	7.23	0.62
5	6.88	0.58
6	6.71	0.57
7	7.15	0.61
8	8.14	0.69
9	9.09	0.77
10	9.73	0.83
15	10.92	0.93
20	11.26	0.96
30	11.51	0.98
40	11.40	0.97
50	11.05	0.94
60	10.88	0.92

Also plotted in Figure 13 and listed in Table 6 are the present recommended TCSs for positron collisions with Kr. Given that the ANU data are corrected for the forward scattering effect, the recommended TCS mostly follows that data set, although it also takes into account the uncertainty in the forward scattering correction. However, below 1 eV where the lowest ANU point is clearly too low, the recommended TCS follows the Trento measurements. Although the latter cross sections are uncorrected for the forward scattering effect, which means that the real TCS is expected to be somewhat larger in magnitude than the Trento results, they currently represent the best TCSs at those very low energies. The recommended TCS is consistent with the measurements of Sinapius et al. [18], Makochekanwa et al. [32], Zecca et al. [180] and Dababneh et al. [178], within its uncertainty range. However, the data of Canter et al. [43,44] and Dababneh et al. [177] lie within that confidence interval only partially (at between 6 and 20 eV and above ∼10 eV, respectively).

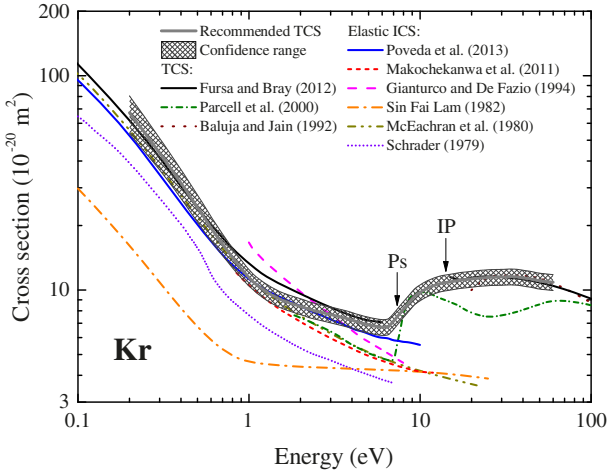

Fig. 14. Computations of the TCS and elastic ICS for positron scattering from krypton. Shown are the TCSs of Fursa and Bray [144], Parcell et al. [170] and Baluja and Jain [71], as well as the elastic ICSs of Poveda et al. [72], Makochekanwa et al. [32] (ROP model), Gianturco and De Fazio [183] (model with $V_{cp}^{(2)}$ with all three coefficients), Sin Fai Lam [182] (un-normalised V_p model), McEachran et al. [181] and Schrader [89]. Also shown is the present recommended TCS and its uncertainty range.

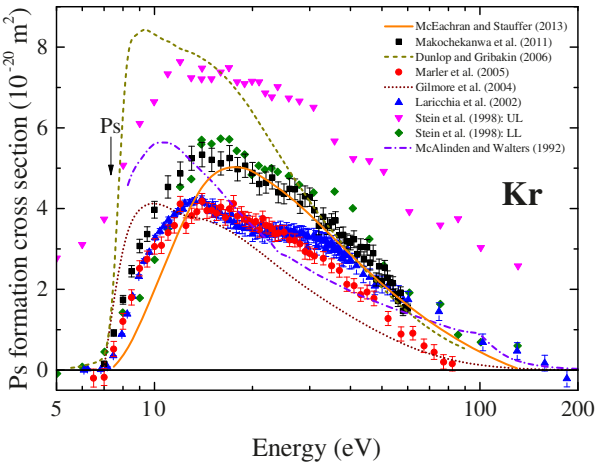

Fig. 15. Experimental and theoretical cross sections for Ps formation in Kr. Shown are the data of Makochekanwa et al. [32], Marler et al. [113], Laricchia et al. [151], and the upper (UL) and lower (LL) bounds reported by Stein et al. [185]. The plotted calculations include those of McAlinden and Walters [92], Gilmore et al. [112], Dunlop and Gribakin [156] and McEachran and Stauffer [155].

On the other hand, the results of Jay and Coleman [179] are entirely outside that uncertainty range.

Figure 14 shows the available calculations of the TCS and elastic ICS for positron scattering from Kr. Baluja and Jain [71] computed the TCS using their complex-optical-potential approach, while Parcell et al. [170] reported the elastic ICS and TCS obtained from their polarized-orbital method and a distorted-wave framework. The CCC formulation was used by Fursa and Bray [144] to also determine the TCS. The most recent calculations of the elastic ICS are due to Poveda et al. [72] with their model-potential approach and Makochekanwa et al. [32] who used their relativistic optical potential model. Theoretical elastic ICSs were also calculated by Gianturco and De Fazio [183] who employed a parameter-free semiclassical model for the polarisation potential, Sin Fai Lam [182] with a normalised and an un-normalised polarisation potential obtained through a procedure based on the Pople-Schofield approximation, McEachran et al. [181] with their frozen-core version of the polarised-orbital approximation, and Schrader [89] based on their simple model for the effects of polarisation.

We observe in Figure 14 a situation similar to Figure 10 for Ar, namely a scatter in the various computed cross sections. The calculated TCSs and elastic ICSs show a somewhat similar qualitative behaviour, but they span a quite large magnitude range. In fact, most of those theoretical results appear to underestimate the two most recent data sets [32,180]. This might be explained, at least in part, by the fact that at the time of the first models of Schrader [89], McEachran et al. [181] and Sin Fai Lam [182] only the earlier measured data of Canter et al. [43,44], Sinapius et al. [18] and Dababneh et al. [177] were available as experimental references. The two most recent computations of Poveda et al. [72] and Fursa and Bray [144] are found to be in very good agreement with the present recommended TCS below the Ps formation threshold. This indicates that there might have been a significant recent advancement in modelling positron-Kr scattering. The level of accord with the result of McEachran et al. [181] is also remarkably good, though only below ∼2 eV. Between the Ps formation threshold and the first ionisation energy, no model offers a good description of the measurements or the recommended TCS. This most likely reflects the difficulty in treating the Ps formation channel from a theoretical point of view. On the other hand, above the first ionisation energy, both the calculations of Fursa and Bray [144] and Baluja and Jain [71] are very good at reproducing the measured TCSs.

5.2 Positronium formation cross section

There have been numerous measurements over the past 30 years looking into Ps formation in Kr [32,97,101,113,151,184,185], whereas most of the theoretical attempts at calculating the cross section for that scattering channel date from more recent times [92,112,155,156]. Figure 15 shows a selection of those experimental studies together with all the above-cited computations. Specifically, shown in Figure 15 are the Ps formation cross sections of Makochekanwa et al. [32] and Marler et al. [113] measured with a buffer-gas trap and positron beam within a strong magnetic field, and those of Stein et al. [185] and Laricchia et al. [151] obtained using mostly electrostatic spectrometers. Note that the cross section of Laricchia et al. [151] was obtained in a similar fashion to Ar (see Sect. 4.2), namely by taking the difference between their measured

total and direct ionisation cross sections and from other existing data. In addition, Stein et al. [185] only reported a range (lower and upper limits) for the Ps formation cross section.

The level of accord among the various measurements plotted in Figure 15 is only qualitative. The range of cross sections, within the limits, by Stein et al. [185] and the data of Makochekanwa et al. [32] are, in general, significantly larger in magnitude than the results of Marler et al. [113] and Laricchia et al. [151]. The two latter experiments are in quantitative agreement, to within the respective error bars, from threshold up to ∼35 eV and they both show an absolute maximum at ∼15 eV. However, the Ps formation cross section of Marler et al. [113] "turns off" at around 80 eV, while that of Laricchia et al. [151] appears to reach a zero magnitude just below ∼200 eV. Moreover, the data by Laricchia et al. [151] appear to be different in shape: they shows a second maximum or, rather, a shoulder at around 25 eV, which is not present in any of the other measurements. Note that we have already seen this behaviour in the UCL data for Ps formation in Ar (Fig. 11). As discussed in detail in Section 4.2, that behaviour might be ascribed to the method employed to extract the Ps formation cross section from their measured total ionisation cross section. An analogous case to Ar might also be made here, as Marler et al. [22] managed to bring the Ps formation data for Kr by Laricchia et al. [151] into agreement with their own [113], simply by subtracting their direct ionisation data from the UCL total ionisation cross sections. We also note in Figure 15 that the ANU data [32] lie above those of Marler et al. [113] and Laricchia et al. [151] at most incident energies, although they merge with the UCL data at ∼40 eV and seem to trend towards the cross section of Marler et al. [113] at higher energies.

The calculations of the Ps formation cross section for Kr shown in Figure 15 are the truncated coupled-static approximation of McAlinden and Walters [92], the DWBA of Gilmore et al. [112], the first-order many-body perturbation theory of Dunlop and Gribakin [156] and the relativistic optical potential approach of McEachran and Stauffer [155] with an additional absorption channel to simulate Ps formation. Those four theories provide quite different cross section shapes and magnitudes from each other and compared to the experimental data. The computations of Gilmore et al. [112] and Dunlop and Gribakin [156] show a much steeper onset of Ps than what the measurements suggest and, together with the model of McAlinden and Walters [92], they predict a maximum in the cross section at around 10 eV, i.e. some 5 eV below the peak in the measured data. The cross section of McEachran and Stauffer [155] is in overall good qualitative agreement with the measurements undertaken at the ANU [32] and that level of accord becomes quantitative at around and above the maximum, i.e. just below 20 eV. We also note that the computation of Dunlop and Gribakin [156] is in good agreement with the model of McEachran and Stauffer [155], as well as the ANU [32] and UCL [151] data at the higher energies (above ∼30 eV).

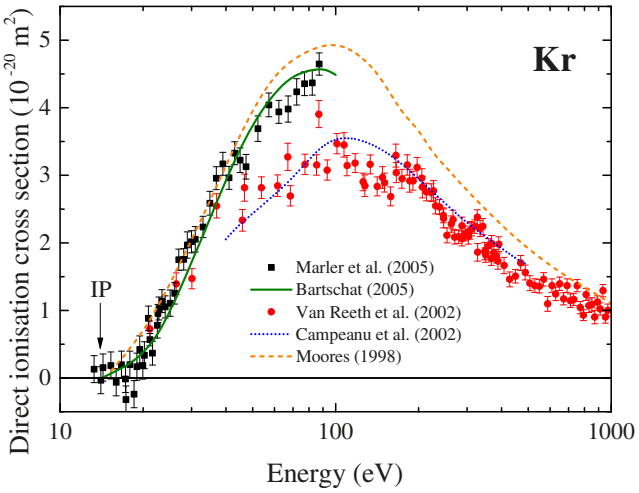

Fig. 16. Direct ionisation cross sections for positron impact with Kr. Shown are the data of Van Reeth et al. [157] and Marler et al. [113], as well as the computations of Moores [160], Campeanu et al. [129] and Bartschat [161].

5.3 Ionisation cross section

Most of the measurements of the direct ionisation cross sections for positron scattering from Kr were undertaken by the UCL group [118,157,158], however for completeness we also mention the work of Marler et al. [113] at the University of California. Total ionisation experiments have also been conducted at UCL [101,151], the University of Aarhus [176] and the University of California [113]. Figure 16 compares the two latest results for the direct ionisation cross sections of Kr, namely that of Van Reeth et al. [157] measured using a mostly electrostatic apparatus and that of Marler et al. [113] with a buffer-gas trap and positron beam in a strong magnetic field.

We observe in Figure 16 that the two experimental data sets are in very good quantitative agreement, however only up to an incident energy of ∼50 eV. Above that energy, the cross section of Marler et al. [113] continues to rise in magnitude, whereas the earlier measurements of Van Reeth et al. [157] reach a plateau at $\sim 3\times10^{-20}$ m^2 and then start to decline in magnitude at ∼200 eV. The data of Van Reeth et al. [157] suggest the presence of a broad maximum centred at ∼100 eV and that the cross section is still non-zero at 1 keV. Given the bigger size and larger number of electrons in Kr compared to Ar (see Tab. 1), one would intuitively expect the ionisation channel to be stronger in the former atom than in the latter. However, by comparing the Kr measurements of Van Reeth et al. [157] with those from the same authors for Ar (Fig. 12), it appears that they in fact might be very similar. Contrary to this, the data of Marler et al. [113] suggest a larger cross section for Kr, which would be consistent with the observed difference in the physico-chemical properties of the heavier noble gases (Tab. 1). Hence, further direct ionisation measurements of Kr would be welcome in order to help clarify the present situation.

While, to the best of our knowledge, only two computations of the total ionisation cross section for Kr exist

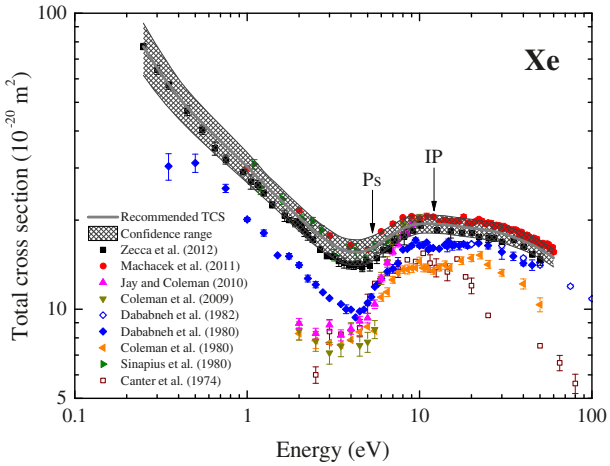

Fig. 17. Comparison of the experimental TCSs for positron interactions with xenon by Canter et al. [44], Sinapius et al. [18], Coleman et al. [162,163], Dababneh et al. [177,178], Jay and Coleman [179], Machacek et al. [33], Zecca et al. [187]. Also shown is the present recommended TCS and its confidence limits.

in references [71,144], quite a few models for direct ionisation have been developed [128–130,160,161,186]. We report in Figure 16 some of those theoretical results, namely the distorted wave calculation with CC target states of Moores [160], the distorted-wave results of Campeanu et al. [129] and the distorted wave computation combined with an R-matrix CC expansion by Bartschat [161]. There is a very good agreement between results from the two models of Moores [160] and Bartschat [161] and the data of Marler et al. [113] at the common energies. The calculation of Campeanu et al. [129], instead, seems to agree very well with the measurements of Van Reeth et al. [157].

6 Xenon

6.1 Total cross section and elastic integral cross section

Xenon is the rarest atom amongst the stable noble gases, which explains the high cost in its production as a high-purity gas. Nonetheless, several TCS measurements have been undertaken over the last four decades or so on that target atom [18,33,44,162,163,177–179,187]. Given its large number of electrons, Xe may be considered a very challenging atom to tackle from a theoretical perspective, as computations might require large computational resources with a fully relativistic target description probably being needed. Despite that, there have been several calculations for positron-Xe scattering [78,83,90,132,171,173,174,179].

Figure 17 presents a comparison of all the existing positron-Xe TCS measurements cited above. The low-energy trend of the positron TCS for Xe looks consistent with the behaviour that one might expect from the stable noble gas with the largest atomic polarisability of the series (see Tab. 1). Namely, we see a dramatic decrease in the TCS from 0.25 eV up to ∼4 eV, followed by an increase in the cross section due to the opening of the Ps formation channel. Somewhat surprisingly, the TCS appears to reach a maximum at around 10 eV, i.e. before the first ionisation energy, and then slowly decreases in magnitude as the incident energy is increased. By comparing Figures 13 and 17 it is apparent that the TCS for the heaviest stable noble gas is significantly larger in magnitude than that of the second heavier gas. This is well consistent with the difference in the main physico-chemical properties of those two atoms (Tab. 1).

The various experimental studies plotted in Figure 17 show, in general, a good qualitative level of accord. Note that only the ANU data [33] are corrected for the forward angle scattering error. The data of Sinapius et al. [18], Machacek et al. [33] and Zecca et al. [187] are very similar in magnitude and, at some energies, some of them are even consistent with each other within the respective overall error bars. However, if elastic DCSs were available to determine the forward scattering correction, those three data sets would become more consistent with each other. All the other results in Figure 17 show a smaller TCS than the three aforementioned data sets and that discrepancy becomes larger as the incident energy is decreased. This observation is consistent with those earlier experiments suffering from a larger forward angle scattering effect, as well as a less precise energy zero determination, compared to the more recent spectrometers at the ANU [33] and the University of Trento [187]. The correction for the forward angle scattering effect is energy dependent and, for most spectrometers, it increases as the impact energy is reduced [56].

We present our recommended TCS for positron scattering from Xe in Figure 17. Tabulated values are also given in Table 7. The recommended TCS mostly follows the ANU data, as that data set is corrected for the forward scattering effect. However, we note that the uncertainty in that correction was also taken into account in the determination of the recommended TCS. Below 1 eV the recommended TCS follows the Trento results, which are uncorrected for the forward scattering effect, but are affected by a much smaller error compared to the Detroit data [177,178]. At those very low energies, we expect the real TCS to be somewhat larger in magnitude than the Trento results. With the exception of the data of Sinapius et al. [18] and the higher-energy (>7 eV) points of Coleman et al. [163] and Jay and Coleman [179], all the other measurements lie well outside the estimated confidence bound on our recommended TCS.

Figure 18 reports the available theoretical TCSs and elastic ICSs for positron-Xe scattering. The TCS calculations include the complex-optical-potential model of Baluja and Jain [71], the polarized-orbital method with distorted-wave framework of Parcell et al. [188] and the CCC formalism of Fursa and Bray [144]. Elastic ICSs have also been determined by Parcell et al. [188] by the polarised-orbital method, Schrader [89] with a simple model for polarisation effects, McEachran et al. [181] using their frozen-core version of the polarised-orbital approximation, Sin Fai Lam [182] with their normalised and

Table 7. Recommended TCSs for positron interaction with Xe.

Energy (eV)	TCS (10^{-20} m^2)	TCS uncertainty (10^{-20} m^2)
0.25	77.14	15.43
0.3	65.32	11.90
0.4	51.89	7.99
0.5	44.59	6.16
0.6	40.33	5.39
0.7	37.04	4.81
0.8	34.41	4.35
0.9	32.24	3.99
1	30.42	3.68
1.5	23.96	2.40
2	20.38	2.04
3	16.84	1.68
4	15.64	1.56
5	15.86	1.59
6	16.83	1.45
7	17.87	1.43
8	18.78	1.50
9	19.27	1.54
10	19.41	1.36
15	19.20	1.34
20	18.83	1.32
30	18.06	1.25
40	17.03	1.19
50	16.03	1.12
60	14.93	1.05

an un-normalised polarisation potential, Gianturco and De Fazio [183] who made use of a parameter-free semi-classical model for the polarisation potential and Poveda et al. [72] with a model-potential approach.

The calculations reported in Figure 18 share a somewhat similar energy dependence below the Ps formation threshold. However, the difference in the magnitude of the various model can be as large as a factor of 4 at the lowest energy shown (0.1 eV). Most of those computations generally underestimate the latest TCS measurements (Fig. 17), although some of them appear to become larger in magnitude than those experimental results at the lowest energies. This would imply a steeper energy dependence of the TCS. However, given the important effect of forward scattering on the measured TCSs at those low energies, it is hard to assess the level of accord between theory and experiment in that energy range. The calculation of Poveda et al. [72] possibly provides the best agreement with the recommended TCS below the Ps formation threshold, while above the first ionisation energy the result of Fursa and Bray [144] compares very well with it. Between those two inelastic thresholds, however, no model appears to reproduce the shape and magnitude of the measured or recommended TCSs.

6.2 Positronium formation cross section

Several experimental investigations of the Ps formation cross section for Xe have been reported in references [33,97,101,113,151,159,185,189] whereas, to the best

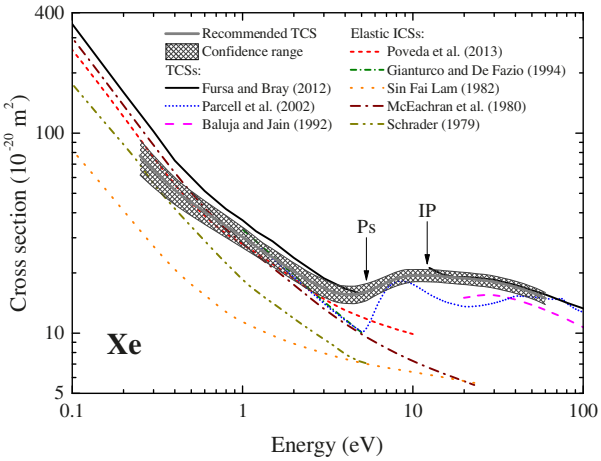

Fig. 18. Theoretical results for positron collisions with xenon. Shown are the TCSs by Baluja and Jain [71], Parcell et al. [188] and Fursa and Bray [144], and the elastic ICSs of Schrader [89], McEachran et al. [181], Sin Fai Lam [182] (with the un-normalised polarisation potential), Gianturco and De Fazio [183] (with $V_{cp}^{(2)}$ with all three coefficients) and Poveda et al. [72]. Also shown is the present recommended TCS and its uncertainty range.

of our knowledge, only four theoretical studies appear to exist [92,112,155,156]. We show in Figure 19 some of those measurements, namely the earlier data of Stein et al. [185] (upper and lower bounds on the cross section only), Laricchia et al. [151], Szłuinska et al. [159] obtained using a mostly electrostatic apparatus and the most recent results of Marler et al. [113] and Machacek et al. [33] gathered employing a buffer-gas trap within a strong magnetic field. As for Ar and Kr, the Ps data measured at UCL [151,159] have been obtained by subtracting previous single and double ionisation cross sections from their total ionisation cross section measurements.

We observe a fair level of accord among the various measurements shown in Figure 19, with most of the experiments showing a similar behaviour and magnitude. Specifically, the Ps formation cross section shows a maximum at around 10 eV with a magnitude of around 9×10^{-20} m^2, that is much larger than all the lighter nobles gases. This is of course in agreement with the trend in the physico-chemical properties of those targets as a function of the atomic number (see Tab. 1). The absolute maximum is then followed by a second peak or broad shoulder just below 20 eV, which is thought to arise from Ps formation by capture of an electron from the 5s inner shell of Xe (threshold energy 16.5 eV) [185]. However, Surko et al. [26] argued that "the origin of this shoulder is still unclear at present". Although we believe that an instrumental artefact might be likely at the origin of this broad shoulder, further, accurate measurements are needed to ascertain the real shape of the cross section at those energies. We also note that the systematic error in the UCL Ps formation data [151,159] found in Ar and Kr might similarly apply here and contribute to produce the double-peaked shape of the Xe TCS. The higher-energy

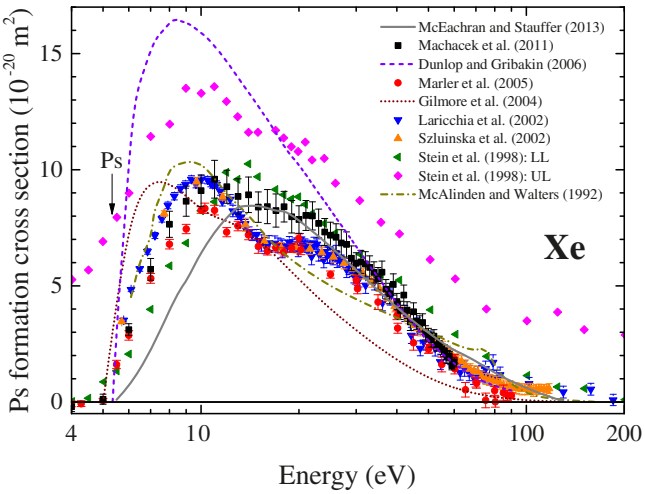

Fig. 19. Ps formation cross sections for positron scattering from Xe. The measurements are by Stein et al. [185], with upper (UL) and lower (LL) limits shown, Laricchia et al. [151], Szłuinska et al. [159], Marler et al. [113] and Machacek et al. [33]. The calculations are from McAlinden and Walters [92], Gilmore et al. [112], Dunlop and Gribakin [156] and McEachran and Stauffer [155].

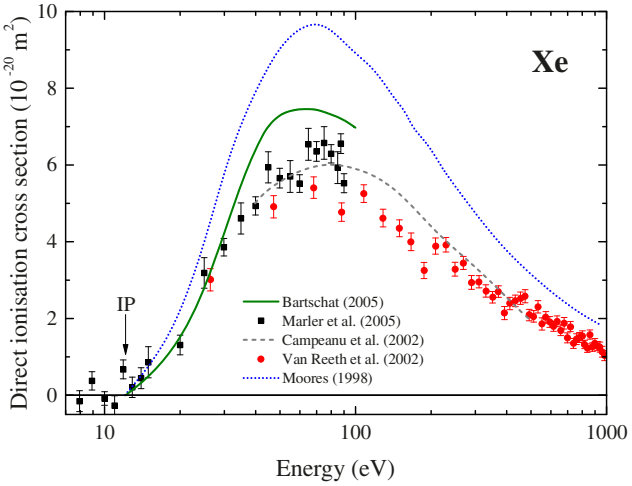

Fig. 20. Direct ionisation cross sections for positron collisions with Xe. The measurements are due to Van Reeth et al. [157] and Marler et al. [113], whereas the calculations are from Moores [160], Campeanu et al. [129] and Bartschat [161].

trend in all the experiments indicates that Ps formation in Xe might "turn off" at between 100 and 200 eV. Figure 19 also clearly shows that the lower bound defined by Stein et al. [185] is possibly too large in magnitude, whereas their upper bound may be considerably overestimated.

The theories for the Ps formation cross section in Xe, that are reported in Figure 19, are the truncated coupled-static approximation of McAlinden and Walters [92], the DWBA of Gilmore et al. [112], the first-order many-body perturbation model of Dunlop and Gribakin [156] and the relativistic optical potential method of McEachran and Stauffer [155] with an additional absorption channel to simulate Ps formation. Similar to Kr (Fig. 15), the various calculations for Xe are quite different in shape and magnitude, with the model of Dunlop and Gribakin [156] being significantly larger than the other three above threshold and at the intermediate energies. The results of McAlinden and Walters [92] are possibly closest to the experiments at around the maximum in the cross section, whereas the calculations of Dunlop and Gribakin [156] and McEachran and Stauffer [155] do a better job at reproducing the higher-energy data. However, only the computation of Gilmore et al. [112] appears to present the "double peaked" shape observed in the measurements.

6.3 Ionisation cross section

In analogy to Kr (see Sect. 5.3), the majority of the direct [157,158] and total [101,151,159] ionisation cross section measurements were conducted at UCL. Nevertheless, we also cite the data of Marler et al. [113], for both cross sections, and Bluhme et al. [124] just for total single (direct ionisation plus Ps formation) and total double (direct double ionisation plus double ionization with Ps formation) ionisation. We compare in Figure 20 the most recent direct ionisation data measured at UCL [157] and the University of California [113]. We see that they are in fair agreement with each other at the common energies and form a complementary data set from threshold up to 1000 eV. Although both measurement show a quite broad maximum at around 70–80 eV, there is a slight difference in the magnitude of that peak. The peak magnitude in Xe is in any case larger than in Kr or the other lighter rare gases.

A large number of calculations of the direct ionisation cross section is also available for Xe [128–130,160,161,186], whereas there appear to be only two theoretical works on the total ionisation cross section [71,144]. Figure 20 displays some of those direct ionisation studies and compares them to the experimental data described above. The plotted theoretical results include the distorted wave computation with CC target states of Moores [160], the distorted-wave model of Campeanu et al. [129] and that same type of approach, but combined with an R-matrix CC expansion, as used by Bartschat [161]. Those cross sections present a similar shape, with a peak between 60 and 80 eV in agreement with the experiments, but different magnitudes. The calculation of Bartschat [161] reproduces the available data pretty well up to ∼30 eV, while that of Campeanu et al. [129] does a fair job at around the maximum and at the higher energies.

7 Other atoms

The only atoms, other than the noble gases, that have been investigated in positron scattering experiments appear to be atomic hydrogen (H), the alkali metals lithium (Li), sodium (Na), potassium (K), rubidium (Rb) and caesium (Cs), and the metal vapour atom magnesium (Mg). Calculations have been performed on those targets and also the heaviest noble gas radon (Rn), the alkaline-earth metals from beryllium (Be) through to radium (Ra),

as well as the two-electron systems zinc (Zn), cadmium (Cd) and mercury (Hg). H is the simplest target to tackle theoretically. However, experimental investigations of atomic H can be challenging, because of the difficulty in producing a target: H beam densities are low even in an attenuation measurement. The alkali-metal atoms enjoyed significant theoretical interest partly because of their relatively simple structure, i.e. a closed shell plus one valence electron [1]. Although an accurate account of electron-positron correlations is more difficult for the alkali and alkaline atoms in comparison to the noble gases, a quite successful theoretical treatment of the scattering problem for those targets has nevertheless been achieved, for instance, by using few-body theory [26]. Moreover, the polarisability of the alkali-metals is much larger than that of the noble gases or any of the other atomic targets measured in positron scattering experiments [1], which makes them even more intriguing to investigate. However, as the alkali and alkaline-metal atoms are solid at room temperature and mostly reactive, scattering measurements on those substances have been hindered for quite some time. Nevertheless, with the development, over a decade and a half ago, of scattering cells that can be heated up to several hundered degress in order to increase the target vapour pressure, attenuation measurements on metallic atoms have become more feasible.

The vast majority of the measurements and computations on all these atomic targets has been carried out prior to the early 2000s and the reader can refer to previous reviews [1,26,190] and references therein for a detailed description of those investigations. Here we just mention the extensive set of total and Ps formation cross section measurements for most of the alkali-metal atoms (see [191] and references therein), Mg [192] and atomic H (see [193] and references therein) by the Wayne State University group using an attenuation technique. An overall comparison of those atomic targets is given by Stein et al. [185]. We note here an interesting feature of positron collisions with the alkali metal atoms, namely that the Ps formation channel is open at all energies, because their first ionisation energy is less than the 6.8 eV binding energy of ground state Ps. Similarly, the ionisation potential of the alkaline metals is slightly bigger than 6.8 eV and, hence, the Ps channel is open at almost all energies. This often results in a Ps formation cross section that is very large at near-threshold energies [192]. Theoretical approaches, such as coupled-channel [194,195], close-coupling [196] and many-body correlation potential [197] methods, provide total and Ps formation cross sections for the alkali atoms (except the heaviest), and the alkaline metal Mg, that are in fair accord with those measured by the Detroit group [191], once corrected for forward angle scattering effects [26].

To the best of our knowledge, no measurements of the positron scattering cross sections for other atomic targets than the noble gases have been conducted after 2004. On the theoretical side of things, some development has occurred since then for H, Mg and the alkali metals. The Curtin University group, in particular, calculated

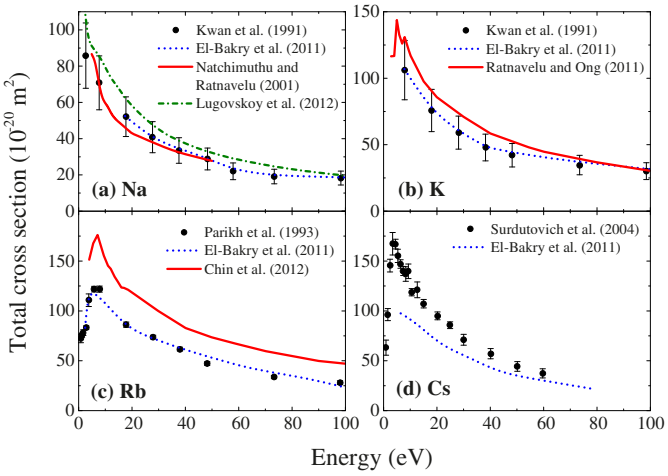

Fig. 21. A selection of the available TCSs for positron scattering from the alkali-metal atoms: (a) Na, (b) K, (c) Rb and (d) Cs. Shown are the measurements of the Wayne State University group [191,205,206], the CCC results of Lugovskoy et al. [202], the GTB calculations of El-Bakry et al. [211], and the CCOM computations of Natchimuthu and Ratnavelu [195] (CCO 5,3), Ratnavelu and Ong [207] and Chin et al. [208] (CCO 8,6).

the near-threshold positron-impact ionisation of atomic H [198] and the H($1s$) formation cross section for Ps-proton scattering [199], which is equivalent to positron-atomic H scattering, utilising the CCC method. The same authors also applied that approach to study the total, elastic, ionisation, electronic excitation and Ps formation cross sections for the lighter alkali metals Li [200,201], Na [201,202] and K [201], as well as Mg [203,204], at low and very low incident energies. Very good qualitative, and at times also quantitative, agreement is found, for instance, between the CCC TCS [202] and the uncorrected (for forward scattering) measurements from the Detroit group [205] for Na (see Fig. 21a). If the experimental data were corrected for the forward angle scattering effect, we might expect the level of accord to improve further, although the extent of that correction is unknown at present. With respect to the alkali metals, the group of Ratnavelu has also recently calculated the elastic ICS, the ICSs for the excitation of various electronic transitions, the Ps formation ICS, the ionisation ICS and the TCS for positron impact with K [207] and Rb [208], at intermediate and high energies, using the coupled-channel optical method (CCOM), which is a fully ab initio model. Those computations are in overall good qualitative, and sometimes also quantitative, agreement with the corresponding uncorrected (for forward scattering) data from the Wayne State University group [205,206] (see Fig. 21). We also mention the work by the group of El-Bakry who employed a relatively new computational technique, known as gradient tree boosting (GTB), to compute the TCS for positron scattering from the Na [209–211], K [209–212], Rb [210,211,213] and Cs [210,211] atoms in the low and intermediate energy regions. Although the GTB method is a machine learning technique and, therefore, not a fully ab initio approach, it appears to provide a good match

to the uncorrected (for forward scattering) experimental data (see Fig. 21), except for Cs. The disagreement observed in Figure 21d simply appears to stem from the fact that the experimental data for positron-Cs scattering shown by El-Bakry et al. [211] in their Figure 3 do not actually match the Detroit data [191]. El-Bakry also applied the same method to obtain the Ps formation cross section for K [212] and Rb [213]. For completeness we also cite the hyperspherical-hidden-crossing calculation of Ward and Shertzer [214] for Ps formation in Li, as well as the optical-model computations of Ke et al. [215] and Guang-Jun et al. [216] for Ps formation in Na and K, respectively.

8 Conclusions

We have reviewed recent progress in the measurements and calculations of the cross sections for low-energy positron scattering from atomic targets. The vast majority of the experiments and theoretical models focussed on the lighter noble gases from He through to Xe, as they are mostly unreactive and easy to handle and because of their closed-shell configurations.

Most of the measurements on those atoms were conducted in the 1970s and '80s, while only a small fraction were carried out within the last 10 years or so. Those recent experiments were carried out with spectrometers characterised by a much better angular discrimination compared to those of 20–40 years ago. This resulted in much smaller forward angle scattering corrections and, therefore, better quality cross sections, such as those measured at the University of Trento and the ANU. The level of accord between the various data sets for the rare gases has consequently noticeably improved. In fact, the measured TCSs for positron-noble gas scattering systems such as He and Ar may now be considered to be largely benchmarked. It is interesting to note that the very-low-energy ($<$1 eV) TCSs for Ar and Kr show a $1/E$ behaviour, while that for Xe exhibits a $1/\sqrt{E}$ energy dependence. The scarcity of data in the TCSs for He and Ne below 1 eV unfortunately prevents us from giving a statement on this behaviour for those two lighter nobles gases.

From the experimental point of view, it is safe to state that in order to achieve an advancement with respect to the latest measurements, future TCS spectrometers shall include substantial technical improvements. The parameters where such improvements are needed, are beam intensity (which, in turn, means positron source intensity), angular resolution at the detector, and extending the low-energy range well below 0.5 eV. An energy range well above a few hundred eV is not considered as a priority, since it is common belief that at high energies the positron cross sections merge with the electron-impact counterpart, which are already relatively well-known. A special mention is the need to search for resonances in positron-atom (and molecule) cross sections. There is a wide theoretical confidence that such resonances exist, although their observation has been hindered so far by the wide beam energy resolution (typically larger than $\sim$0.3 eV FWHM, except for the magnetized buffer-gas trap and positron beam spectrometers) and low beam intensity of the existing experiments, as well as the restraining nature of the atoms predicted to bind positrons. Future positron spectrometers with both better energy resolution and higher beam intensity might, therefore, be used to search for such resonances.

On the theoretical side of things, significant developments in the computations of the TCS and elastic ICS have been observed for most of the noble gases, particularly using convergent close-coupling and model-potential approaches. Nonetheless, further progress still appears to be required in order to reach a closer agreement with the experiments. Some scatter among the most recent experimental data and, to a larger extent, calculations of the Ps formation and ionisation cross sections was found for all the noble gases except He. This observation suggests that additional measurements and theoretical developments may be warranted in order to improve the current situation and better ascertain the shape and magnitude of those cross sections. A theoretical search for resonances might run in parallel with a similar experimental exploration.

Most of the positron scattering investigations on atoms other than the nobles gases have been devoted to atomic hydrogen, the alkali and alkaline metals, and atoms that can be considered two-electron systems. However, it appears that no recent experiments have been conducted on those targets. Hence, new, high-resolution, high-accuracy measurements would be very useful. Computations of the TCS and Ps formation cross sections for H, Mg and the alkali-metal atoms have been carried out since 2004 using the CCC, CCOM and GTB approaches. A relatively good match to earlier measurements for those scattering systems was found with these methods. Nevertheless, there is a need for further ab initio quality calculations, particularly on more challenging atomic targets, such as the alkaline-earth metals.

The authors would like to thank Robert P. McEachran, Dmitry V. Fursa and Igor Bray for making their numerical files available. L.C. acknowledges the Australian Research Council through its Centres of Excellence Program for financial support.

References

1. W.E. Kauppila, T.S. Stein, in *Advances in Atomic, Molecular, and Optical Physics* (Academic Press, San Diego, 1990), Vol. 26, p. 1
2. C. Ramsauer, Ann. Phys. **64**, 513 (1921)
3. J.S. Townsend, V.A. Bailey, Philos. Mag. **43**, 593 (1922)
4. A. Zecca, G.P. Karwasz, R.S. Brusa, Riv. Nuovo Cimento **19**, 1 (1996)
5. M. Charlton, J.W. Humberston, *Positron Physics* (Cambridge University Press, Cambridge, 2001)
6. G.J. Schulz, Rev. Mod. Phys. **45**, 378 (1973)
7. J.A. Young, C.M. Surko, Phys. Rev. A **77**, 052704 (2008)
8. J.A. Young, C.M. Surko, Phys. Rev. A **78**, 032702 (2008)

9. J.R. Danielson, J.A. Young, C.M. Surko, J. Phys.: Conf. Ser. **199**, 012012 (2010)
10. J. Mitroy, M.W.J. Bromley, G.G. Ryzhikh, J. Phys. B **35**, R81 (2002)
11. P.H.R. Amaral, J.R. Mohallem, Phys. Rev. A **86**, 042708 (2012)
12. C. Harabati, V.A. Dzuba, V.V. Flambaum, Phys. Rev. A **89**, 022517 (2014)
13. D.G. Costello, D.E. Groce, D.F. Herring, J.W.M. McGowan, Can. J. Phys. **50**, 23 (1972)
14. K.F. Canter, P.G. Coleman, T.C. Griffith, G.R. Heyland, J. Phys. B **5**, L167 (1972)
15. B.H. Bransden, P.K. Hutt, J. Phys. B **8**, 603 (1975)
16. A.G. Brenton, J. Dutton, F.M. Harris, J. Phys. B **11**, L15 (1978)
17. W.E. Kauppila, T.S. Stein, G. Jesion, Phys. Rev. Lett. **36**, 580 (1976)
18. G. Sinapius, W. Raith, W.G. Wilson, J. Phys. B **13**, 4079 (1980)
19. P.G. Coleman, J.T. Hutton, Phys. Rev. Lett. **45**, 2017 (1980)
20. O. Sueoka, S. Mori, J. Phys. Soc. Jpn **53**, 2491 (1984)
21. O. Sueoka, A. Hamada, J. Phys. Soc. Jpn **62**, 2669 (1993)
22. J.P. Marler, L.D. Barnes, S.J. Gilbert, J.P. Sullivan, J.A. Young, C.M. Surko, Nucl. Instrum. Methods Phys. Res. B **221**, 84 (2004)
23. A. Zecca, C. Perazzolli, M.J. Brunger, J. Phys. B **38**, 2079 (2005)
24. J.P. Sullivan, C. Makochekanwa, A. Jones, P. Caradonna, S.J. Buckman, J. Phys. B **41**, 081001 (2008)
25. C.M. Surko, in *New Directions in Antimatter Chemistry and Physics*, edited by C.M. Surko, F.A. Gianturco (Kluwer, Dordrecht, 2001), p. 345
26. C.M. Surko, G.F. Gribakin, S.J. Buckman, J. Phys. B **38**, R57 (2005)
27. T.C. Griffith, G.R. Heyland, Phys. Rep. **39**, 169 (1978)
28. A.S. Ghosh, N.C. Sil, P. Mandal, Phys. Rep. **87**, 313 (1982)
29. T.S. Stein, W.E. Kauppila, in *Advances in Atomic and Molecular Physics*, edited by D. Bates, B. Bederson (Academic Press, New York, 1982), Vol. 18, p. 53
30. M. Charlton, in *New Directions in Antimatter Chemistry and Physics*, edited by C.M. Surko, F.A. Gianturco (Kluwer, Dordrecht, 2001), p. 223
31. P. Caradonna, J.P. Sullivan, A. Jones, C. Makochekanwa, D. Slaughter, D.W. Mueller, S.J. Buckman, Phys. Rev. A **80**, 060701(R) (2009)
32. C. Makochekanwa, J.R. Machacek, A.C.L. Jones, P. Caradonna, D.S. Slaughter, R.P. McEachran, J.P. Sullivan, S.J. Buckman, S. Bellm, B. Lohmann, D.V. Fursa, I. Bray, D.W. Mueller, A.D. Stauffer, M. Hoshino, Phys. Rev. A **83**, 032721 (2011)
33. J.R. Machacek, C. Makochekanwa, A.C.L. Jones, P. Caradonna, D.S. Slaughter, R.P. McEachran, J.P. Sullivan, S.J. Buckman, S. Bellm, B. Lohmann, D.V. Fursa, I. Bray, D.W. Mueller, A.D. Stauffer, New J. Phys. **13**, 125004 (2011)
34. S.J. Gilbert, R.G. Greaves, C.M. Surko, Phys. Rev. Lett. **82**, 5032 (1999)
35. S.J. Gilbert, J. Sullivan, R.G. Greaves, C.M. Surko, Nucl. Instrum. Methods Phys. Res. B **171**, 81 (2000)
36. J.P. Sullivan, J.P. Marler, S.J. Gilbert, S.J. Buckman, C.M. Surko, Phys. Rev. Lett. **87**, 073201 (2001)
37. J.P. Sullivan, S.J. Gilbert, J.P. Marler, R.G. Greaves, S.J. Buckman, C.M. Surko, Phys. Rev. A **66**, 042708 (2002)
38. J.P. Sullivan, S.J. Gilbert, J.P. Marler, L.D. Barnes, S.J. Buckman, C.M. Surko, Nucl. Instrum. Methods Phys. Res. B **192**, 3 (2002)
39. L.D. Barnes, J.P. Marler, J.P. Sullivan, C.M. Surko, Phys. Scr. T **110**, 280 (2004)
40. J.P. Marler, C.M. Surko, R.P. McEachran, A.D. Stauffer, Phys. Rev. A **73**, 064702 (2006)
41. A.C.L. Jones, P. Caradonna, C. Makochekanwa, D.S. Slaughter, R.P. McEachran, J.R. Machacek, J.P. Sullivan, S.J. Buckman, Phys. Rev. Lett. **105**, 073201 (2010)
42. P.G. Coleman, N. Cheesman, E.R. Lowry, Phys. Rev. Lett. **102**, 173201 (2009)
43. K.F. Canter, P.G. Coleman, T.C. Griffith, G.R. Heyland, J. Phys. B **6**, L201 (1973)
44. K.F. Canter, P.G. Coleman, T.C. Griffith, G.R. Heyland, Appl. Phys. **3**, 249 (1974)
45. B. Jaduszliwer, W.M.C. Keever, D.A.L. Paul, Can. J. Phys. **50**, 1414 (1972)
46. B. Jaduszliwer, D.A.L. Paul, Can. J. Phys. **51**, 1565 (1973)
47. B. Jaduszliwer, D.A.L. Paul, Can. J. Phys. **52**, 1047 (1974)
48. B. Jaduszliwer, A. Nakashima, D.A.L. Paul, Can. J. Phys. **53**, 962 (1975)
49. P.G. Coleman, T.C. Griffith, G.R. Heyland, T.R. Twomey, Appl. Phys. **11**, 321 (1976)
50. J.R. Burciaga, P.G. Coleman, L.M. Diana, J.D. McNutt, J. Phys. B **10**, L569 (1977)
51. A.G. Brenton, J. Dutton, F.M. Harris, R.A. Jones, D.M. Lewis, J. Phys. B **10**, 2699 (1977)
52. W.G. Wilson, J. Phys. B **11**, L629 (1978)
53. T.S. Stein, W.E. Kauppila, V. Pol, J.H. Smart, G. Jesion, Phys. Rev. A **17**, 1600 (1978)
54. P.G. Coleman, J.D. McNutt, L.M. Diana, J.R. Burciaga, Phys. Rev. A **20**, 145 (1979)
55. T.C. Griffith, G.R. Heyland, K.S. Lines, T.R. Twomey, Appl. Phys. **19**, 431 (1979)
56. W.E. Kauppila, T.S. Stein, J.H. Smart, M.S. Dababneh, Y.K. Ho, J.P. Downing, V. Pol, Phys. Rev. A **24**, 725 (1981)
57. T. Mizogawa, Y. Nakayama, T. Kawaratami, M. Tosaki, Phys. Rev A **31**, 2171 (1985)
58. P. Caradonna, A. Jones, C. Makochekanwa, D.S. Slaughter, J.P. Sullivan, S.J. Buckman, I. Bray, D.V. Fursa, Phys. Rev. A **80**, 032710 (2009)
59. K. Nagumo, Y. Nitta, M. Hoshino, H. Tanaka, Y. Nagashima, J. Phys. Soc. Jpn **80**, 064301 (2011)
60. G.P. Karwasz, D. Pliszka, A. Zecca, R.S. Brusa, Nucl. Instrum. Methods Phys. Res. B **240**, 666 (2005)
61. G.P. Karwasz, M. Barozzi, M. Bettonte, R.S. Brusa, A. Zecca, Nucl. Instrum. Methods Phys. Res. B **171**, 178 (2000)
62. A. Zecca, Nucl. Instrum. Methods Phys. Res. B **251**, 517 (2006)
63. G.P. Karwasz, R.S. Brusa, D. Pliszka, Nucl. Instrum. Methods Phys. Res. B **251**, 520 (2006)
64. S.G. Kukolich, Am. J. Phys. **36**, 701 (1968)
65. L.I. Schiff, *Quantum Mechanics* (McGraw-Hill, New York, 1949)
66. V.A. Bailey, J.S. Townsend, Phil. Mag. **46**, 657 (1923)

67. R. Utamuratov, A.S. Kadyrov, D.V. Fursa, I. Bray, A.T. Stelbovics, J. Phys. B **43**, 125203 (2010)
68. Y.-J. Cheng, Y.-J. Zhou, Chin. Phys. Lett. **24**, 3408 (2007)
69. P. Van Reeth, J.W. Humberston, J. Phys. B **32**, 3651 (1999)
70. C.P. Campbell, M.T. McAlinden, A.A. Kernoghan, H.R.J. Walters, Nucl. Instrum. Methods Phys. Res. B **143**, 41 (1998)
71. K.L. Baluja, A. Jain, Phys. Rev. A **46**, 1279 (1992)
72. L.A. Poveda, A. Dutra, J.R. Mohallem, Phys. Rev. A **87**, 052702 (2013)
73. E. Ficocelli Varracchio, J. Phys. B **23**, L109 (1990)
74. J.P. Sullivan, C. Makochekanwa, A. Jones, P. Caradonna, D.S. Slaughter, J. Machacek, R.P. McEachran, D.W. Mueller, S.J. Buckman, J. Phys. B **44**, 035201 (2011)
75. H.S.W. Massey, J. Lawson, D.G. Thompson, in *Quantum Theory of Atoms, Molecules and the Solid State, A Tribute to John C. Slater*, edited by P.-O. Löwdin (Academic Press, New York, 1966), p. 203
76. R.J. Drachman, Phys. Rev. **144**, 25 (1966)
77. M. Kraidy, Ph.D. thesis, University of Western Ontario, 1967
78. J. Callaway, R.W. LaBahn, R.T. Pu, W.M. Duxler, Phys. Rev. **168**, 12 (1968)
79. M.F. Fels, H. Mittleman, Phys. Rev. **182**, 77 (1969)
80. B.D. Buckley, H.R.J. Walters, J. Phys. B **7**, 1380 (1974)
81. H. Aulenkamp, P. Heiss, E. Wichmann, Z. Phys. **268**, 213 (1974)
82. R.I. Campeanu, J.W. Humberston, J. Phys. B **8**, L244 (1975)
83. M. Pai, P. Hewson, E. Vogt, D.M. Schrader, Phys. Lett. A **56**, 169 (1976)
84. M.Ya. Amusia, N.A. Cherepkov, L.V. Chernysheva, S.G. Shapiro, J. Phys. B **9**, L531 (1976)
85. R.P. McEachran, A.G. Ryman, A.D. Stauffer, D.L. Morgan, J. Phys. B **10**, 663 (1977)
86. R.I. Campeanu, J.W. Humberston, J. Phys. B **10**, L153 (1977)
87. J.W. Humberston, J. Phys. B **11**, L343 (1978)
88. J.W. Humberston, in *Advances in Atomic and Molecular Physics*, edited by D.R. Bates, B. Bederson (Academic Press, New York, 1979), Vol. 15, p. 101
89. D.M. Schrader, Phys. Rev. A **20**, 918 (1979)
90. S.L. Willis, J. Hata, M.R.C. McDowell, C.J. Joachain, F.W. Byron Jr., J. Phys. B **14**, 2687 (1981)
91. S.L. Willis, M.R.C. McDowell, J. Phys. B **15**, L31 (1982)
92. M.T. McAlinden, H.R.J. Walters, Hyperfine Interact. **73**, 65 (1992)
93. H. Wu, I. Bray, D. Fursa, A.T. Stelbovics, J. Phys. B **37**, 1165 (2004)
94. H. Wu, I. Bray, D. Fursa, A.T. Stelbovics, J. Phys. B **37**, L1 (2004)
95. T.C. Griffith, G.R. Heyland, K.S. Lines, T.R. Twomey, J. Phys. B **12**, L747 (1979)
96. L.S. Fornari, L.M. Diana, P.G. Coleman, Phys. Rev. Lett. **51**, 2276 (1983)
97. M. Charlton, G. Clark, T.C. Griffith, G.R. Heyland, J. Phys. B **16**, L465 (1983)
98. L.M. Diana, P.G. Coleman, D.L. Brooks, P.K. Pendleton, D.M. Norman, Phys. Rev. A **34**, 2731 (1986)
99. D. Fromme, G. Kruse, W. Raith, G. Sinapius, Phys. Rev. Lett. **57**, 3031 (1986)
100. N. Overton, R.J. Mills, P.G. Coleman, J. Phys. B **26**, 3951 (1993)
101. J. Moxom, G. Laricchia, M. Charlton, A. Kover, W.E. Meyerhof, Phys. Rev. A **50**, 3129 (1994)
102. D.J. Murtagh, M. Szluinska, J. Moxom, P. Van Reeth, G. Laricchia, J. Phys. B **38**, 3857 (2005)
103. P. Mandal, S. Guha, N.C. Sil, J. Phys. B **12**, 2913 (1979)
104. P. Mandal, S. Guha, N.C. Sil, Phys. Rev. A **22**, 2623 (1980)
105. P. Khan, A. S. Ghosh, Phys. Rev. A **28** 2181 (1983)
106. P. Khan, P.S. Mazumdar, A.S. Ghosh, J. Phys. B **17**, 4785 (1984)
107. M. Basu, P.S. Mazumdar, A.S. Ghosh, J. Phys. B **18**, 369 (1985)
108. P. Khan, P.S. Mazumdar, A.S. Ghosh, Phys. Rev. A **31**, 1405 (1985)
109. D.R. Schultz, R.E. Olson, Phys. Rev. A **38**, 1866 (1988)
110. A. Igarashi, N. Toshima, Phys. Lett. A **164**, 70 (1992)
111. R.N. Hewitt, C.J. Noble, B.H. Bransden, J. Phys. B **25**, 557 (1992)
112. S. Gilmore, J.E. Blackwood, H.R.J. Walters, Nucl. Instrum. Methods Phys. Res. B **221**, 129 (2004)
113. J.P. Marler, J.P. Sullivan, C.M. Surko, Phys. Rev. A **71**, 022701 (2005)
114. H. Knudsen, L. Brun-Nielsen, M. Charlton, M.R. Poulsen, J. Phys. B **23**, 3955 (1990)
115. S. Mori, O. Sueoka, J. Phys. B **27**, 4349 (1994)
116. O. Sueoka, B. Jin, A. Hamada, Appl. Surf. Sci. **85**, 59 (1995)
117. F.M. Jacobsen, N.P. Frandsen, H. Knudsen, U. Mikkelsen, D.M. Schrader, J. Phys. B **28**, 4691 (1995)
118. J. Moxom, P. Ashley, G. Laricchia, Can. J. Phys. **74**, 367 (1996)
119. P. Ashley, J. Moxom, G. Laricchia, Phys. Rev. Lett. **77**, 1250 (1996)
120. O. Sueoka, J. Phys. Soc. Jpn **51**, 3757 (1982)
121. S. Mori, O. Sueoka, At. Coll. Res. Jpn **10**, 8 (1984)
122. L.M. Diana, L.S. Fornari, S.C. Sharma, P.K. Pendleton, P.G. Coleman, in *Positron Annihilation*, edited by P.C. Jain, R.M. Singru, K.P. Gopinathan (World Scientific, Singapore, 1985), p. 342
123. J. Moxom, G. Laricchia, M. Charlton, J. Phys. B **26**, L367 (1993)
124. H. Bluhme, H. Knudsen, J.P. Merrison, K.A. Nielsen, J. Phys. B **32**, 5237 (1999)
125. R.I. Campeanu, R.P. McEachran, A.D. Stauffer, J. Phys. B **20**, 1635 (1987)
126. R.I. Campeanu, D. Fromme, G. Kruse, R.P. McEachran, L.A. Parcell, W. Raith, G. Sinapius, A.D. Stauffer, J. Phys. B **20**, 3557 (1987)
127. R.I. Campeanu, R.P. McEachran, A.D. Stauffer, Can. J. Phys. **74**, 544 (1996)
128. R.I. Campeanu, R.P. McEachran, A.D. Stauffer, Can. J. Phys. **79**, 1231 (2001)
129. R.I. Campeanu, R.P. McEachran, A.D. Stauffer, Nucl. Instrum. Methods Phys. Res. B **192**, 146 (2002)
130. R.I. Campeanu, L. Nagy, A.D. Stauffer, Can. J. Phys. **81**, 919 (2003)
131. K. Ratnavelu, Aust. J. Phys. **44**, 265 (1991)
132. Z. Chen, A.Z. Msezane, Phys. Rev. A **49**, 1752 (1994)
133. W. Ihra, J.H. Macek, F. Mota-Furtado, P.F. O'Mahony, Phys. Rev. Lett. **78**, 4027 (1997)

134. D.L. Moores, Nucl. Instrum. Methods Phys. Res. B **179**, 316 (2001)
135. N.C. Deb, D.S.F. Crothers, J. Phys. B **35**, L85 (2002)
136. T.Y. Kuo, H.L. Sun, K.N. Huang, Phys. Rev. A **67**, 012705 (2003)
137. H. Wu, I. Bray, D.V. Fursa, A.T. Stelbovics, J. Phys. B **37**, 1164 (2004)
138. B. Jaduszliwer, D.A.L. Paul, Can. J. Phys. **52**, 272 (1974)
139. B. Jaduszliwer, D.A.L. Paul, Appl. Phys. **3**, 281 (1974)
140. J.-S. Tsai, L. Lebow, D.A.L. Paul, Can. J. Phys. **54**, 1741 (1976)
141. M. Charlton, G. Laricchia, T.C. Griffith, G.L. Wright, G.R. Heyland, J. Phys. B **17**, 4945 (1984)
142. A.C.L. Jones, C. Makochekanwa, P. Caradonna, D.S. Slaughter, J.R. Machacek, R.P. McEachran, J.P. Sullivan, S.J. Buckman, A.D. Stauffer, I. Bray, D.V. Fursa, Phys. Rev. A **83**, 032701 (2011)
143. K. Nagumo, Y. Nitta, M. Hoshino, H. Tanaka, Y. Nagashima, Eur. Phys. J. D **66**, 81 (2012)
144. D.V. Fursa, I. Bray, New J. Phys. **14**, 035002 (2012)
145. D. Assafrão, H.R.J. Walters, F. Arretche, A. Dutra, J.R. Mohallem, Phys. Rev. A **84**, 022713 (2011)
146. V.A. Dzuba, V.V. Flambaum, G.F. Gribakin, W.A. King, J. Phys. B **29**, 3151 (1996)
147. H. Nakanishi, D.M. Schrader, Phys. Rev. A **34**, 1823 (1986)
148. R.I. Campeanu, J. Dubau, J. Phys. B **11**, L567 (1978)
149. R.P. McEachran, A.G. Ryman, A.D. Stauffer, J. Phys. B **11**, 551 (1978)
150. E.S. Gillespie, D.G. Thompson, J. Phys. B **8**, 2858 (1975)
151. G. Laricchia, P. Van Reeth, M. Szluinska, J. Moxom, J. Phys. B **35**, 2525 (2002)
152. B. Jin, S. Miyamoto, O. Sueoka, A. Hamada, At. Coll. Res. Jpn **20**, 9 (1994)
153. L.M. Diana, in *Proceedings of the 7th International Conference on Positron Annihilation*, edited by P. Jain, R.M. Singru, K.P. Gopinathan (World Scientific, Singapore, 1985), p. 428
154. E.S. Gillespie, D.G. Thompson, J. Phys. B **10**, 3543 (1977)
155. R.P. McEachran, A.D. Stauffer, J. Phys. B **46**, 075203 (2013)
156. L.J.M. Dunlop, G.F. Gribakin, Nucl. Instrum. Methods Phys. Res. B **247**, 61 (2006)
157. P. Van Reeth, M. Szłuinska, G. Laricchia, Nucl. Instrum. Methods Phys. Res. B **192**, 220 (2002)
158. V. Kara, K. Paludan, J. Moxom, P. Ashley, G. Laricchia, J. Phys. B **30**, 3933 (1997)
159. M. Szłuinska, P. Van Reeth, G. Laricchia, Nucl. Instrum. Methods Phys. Res. B **192**, 215 (2002)
160. D.L. Moores, Nucl. Instrum. Methods Phys. Res. B **143**, 105 (1998)
161. K. Bartschat, Phys. Rev. A **71**, 032718 (2005)
162. P.G. Coleman, J.D. McNutt, L.M. Diana, J.T. Hutton, Phys. Rev. A **22**, 2290 (1980)
163. P.G. Coleman, N. Cheesman, E.R. Lowry, Phys. Rev. Lett. **102**, 173201 (2009)
164. A. Zecca, L. Chiari, E. Trainotti, D.V. Fursa, I. Bray, A. Sarkar, S. Chattopadhyay, K. Ratnavelu, M.J. Brunger, J. Phys. B **45**, 015203 (2012)
165. R.E. Montgomery, R.W. LaBahn, Can. J. Phys. **48**, 1288 (1970)
166. R.P. McEachran, A.G. Ryman, A.D. Stauffer, J. Phys. B **12**, 1031 (1979)
167. S.K. Datta, S.K. Mandal, P. Khan, A.S. Ghosh, Phys. Rev. A **32**, 633 (1985)
168. A. Jain, Phys. Rev. A **41**, 2437 (1990)
169. S.N. Nahar, J.M. Wadehra, Phys. Rev. A **43**, 1275 (1991)
170. L.A. Parcell, R.P. McEachran, A.D. Stauffer, Nucl. Instrum. Methods Phys. Res. B **171**, 113 (2000)
171. R.P. McEachran, J.P. Sullivan, S.J. Buckman, M.J. Brunger, M.C. Fuss, A. Muñoz, F. Blanco, R.D. White, Z. Lj Petroviæ, P. Limão-Vieira, G. García, J. Phys. B **45**, 045207 (2012)
172. S. Zhou, S.P. Parikh, W.E. Kauppila, C.K. Kwan, D. Lin, A. Surdutovich, T.S. Stein, Phys. Rev. Lett. **73**, 236 (1994)
173. A. Zecca, L. Chiari, A. Sarkar, M.J. Brunger, New J. Phys. **13**, 115001 (2011)
174. L.M. Diana, P.G. Coleman, D.L. Brooks, P.K. Pendleton, D.M. Norman, B.E. Seay, S.C. Sharma, in *Proceedings of the Third International Workshop on Positron (Electron) – Gas Scattering*, edited by W.E. Kauppila, T.S. Stein, J.M. Wadehra (World Scientific, Singapore, 1986), p. 296
175. T.S. Stein, W.E. Kauppila, C.K. Kwan, S.P. Parik, S. Zhou, Hyperfine Interact. **73**, 53 (1992)
176. H. Bluhme, H. Knudsen, J.P. Merrison, K. A. Nielsen, J. Phys. B **32**, 5835 (1999)
177. M.S. Dababneh, W.E. Kauppila, J.P. Downing, F. Laperriere, V. Pol, J.H. Smart, T.S. Stein, Phys. Rev. A **22**, 1872 (1980)
178. M.S. Dababneh, Y.-F. Hsieh, W.E. Kauppila, V. Pol, T.S. Stein, Phys. Rev. A **26**, 1252 (1982)
179. P.M. Jay, P.G. Coleman, Phys. Rev. A **82**, 012701 (2010)
180. A. Zecca, L. Chiari, E. Trainotti, D.V. Fursa, I. Bray, M.J. Brunger, Eur. Phys. J. D **64**, 317 (2011)
181. R.P. McEachran, A.D. Stauffer, L.E.M. Campbell, J. Phys. B **13**, 1281 (1980)
182. L.T. Sin Fai Lam, J. Phys. B **15**, 143 (1982)
183. F.A. Gianturco, D. De Fazio, Phys. Rev. A **50**, 4819 (1994)
184. L.M. Diana, P.G. Coleman, D.L. Brooks, R.L. Chaplin, in *Atomic Physics with Positrons*, edited by J.W. Humberston, E.A.G. Armour (Plenum, New York, 1987), p. 55
185. T.S. Stein, M. Harte, J. Jiang, W.E. Kauppila, C.K. Kwan, H. Li, S. Zhou, Nucl. Instrum. Methods Phys. Res. B **143**, 68 (1998)
186. R.I. Campeanu, R.P. McEachran, A.D. Stauffer, Can. J. Phys. **77**, 769 (1999)
187. A. Zecca, L. Chiari, E. Trainotti, M.J. Brunger, J. Phys. B **45**, 085203 (2012)
188. L.A. Parcell, R.P. McEachran, A.D. Stauffer, Nucl. Instrum. Methods Phys. Res. B **192**, 180 (2002)
189. L.M. Diana, D.L. Brooks, P.G. Coleman, R.L. Chaplin, J.P. Howell, in *Positron Annihilation*, edited by L. Dorokins-Vanpraet, M. Dorokins, D. Segers (World Scientific, Singapore, 1989), p. 311
190. H.R.J. Walters, S. Sahoo, S. Gilmore, Nucl. Instrum. Methods Phys. Res. B **233**, 78 (2005)
191. E. Surdutovich, W.E. Kauppila, C.K. Kwan, E.G. Miller, S.P. Parikh, K.A. Price, T.S. Stein, Nucl. Instrum. Methods Phys. Res. B **221**, 97 (2004)
192. E. Surdutovich, M. Harte, W.E. Kauppila, C.K. Kwan, T.S. Stein, Phys. Rev. A **68**, 022709 (2003)

193. S. Zhou, H. Li, W.E. Kauppila, C.K. Kwan, T.S. Stein, Phys. Rev. A **55**, 361 (1997)
194. M.T. McAlinden, A.A. Kernoghan, H.R.J. Walters, J. Phys. B **29**, 555 (1996)
195. N. Natchimuthu, K. Ratnavelu, Phys. Rev. A **63**, 052707 (2001)
196. R.N. Hewitt, C.J. Noble, B.H. Bransden, C.J. Joachain, Can. J. Phys. **74**, 559 (1996)
197. G.F. Gribakin, W.A. King, Can. J. Phys. **74**, 449 (1996)
198. A.S. Kadyrov, I. Bray, A.T. Stelbovics, Phys. Rev. Lett. **98**, 263202 (2007)
199. A.S. Kadyrov, A.V. Lugovskoy, R. Utamuratov, I. Bray, Phys. Rev. A **87**, 060701 (2013)
200. A.V. Lugovskoy, A.S. Kadyrov, I. Bray, A.T. Stelbovics, Phys. Rev. A **82**, 062708 (2010)
201. A.V. Lugovskoy, R. Utamuratov, A.S. Kadyrov, A.T. Stelbovics, I. Bray, Phys. Rev. A **87**, 042708 (2013)
202. A.V. Lugovskoy, A.S. Kadyrov, I. Bray, A.T. Stelbovics, Phys. Rev. A **85**, 034701 (2012)
203. J.S. Savage, D.V. Fursa, I. Bray, Phys. Rev. A **83**, 062709 (2011)
204. R. Utamuratov, D.V. Fursa, A.S. Kadyrov, A.V. Lugovskoy, J.S. Savage, I. Bray, Phys. Rev. A **86**, 062702 (2012)
205. C.K. Kwan, W.E. Kauppila, R.A. Lukaszew, S.P. Parikh, T.S. Stein, Y.J. Wan, M.S. Dababneh, Phys. Rev. A **44**, 1620 (1991)
206. S.P. Parikh, W.E. Kauppila, C.K. Kwan, R.A. Lukaszew, D. Przybyla, T.S. Stein, S. Zhou, Phys. Rev. A **47**, 1535 (1993)
207. K. Ratnavelu, W.E. Ong, Eur. Phys. J. D **64**, 269 (2011)
208. J.H. Chin, K. Ratnavelu, Y. Zhou, Eur. Phys. J. D **66**, 82 (2012)
209. S.Y. El-Bakry, M.Y. El-Bakry, Indian J. Phys. **78**, 1313 (2004)
210. S.Y. El-Bakry, A. Radi, Int. J. Mod. Phys. C **18**, 351 (2007)
211. S.Y. El-Bakry, E.S. El-Dahshan, M.Y. El-Bakry, Indian J. Phys. **85**, 1405 (2011)
212. S.Y. El-Bakry, Mod. Phys. Lett. B **21**, 625 (2007)
213. S.Y. El-Bakry, Int. J. Mod. Phys. B **21**, 221 (2007)
214. S.J. Ward, J. Shertzer, Nucl. Instrum. Methods Phys. Res. B **221**, 206 (2004)
215. Y. Ke, Y. Zhou, G. Nan, Phys. Rev. A **70**, 024702 (2004)
216. N. Guang-Jun, Z. Ya-Jun, K. You-Qi, Chin. Phys. Lett. **21**, 2406 (2004)